DESIGN AND STUDY OF FLAPPING MECHANISM

WITH ASYMMETRIC FREQUENCIES

by

Sohail Iqbal

2009-NUST-MS PHD- MECH-15

MS-60(MECH)

Submitted to the Department of Mechanical Engineering in fulfillment of the

requirements for the degree of

MASTER OF SCIENCE

in

MECHANICAL ENGINEERING

Thesis Supervisor

Dr M Afzaal Malik

College of Electrical & Mechanical Engineering

National University of Sciences & Technology

2012

بسم الله الرحمن الرحيم

In the name of Allah, the most

Beneficent and the most Merciful

DECLARATION

I hereby declare that I have developed this thesis entirely on the basis of my personal efforts under the sincere guidance of Dr.M Afzaal Malik. All the sources used in this thesis have been cited and the contents of this thesis have not been plagiarized. No portion of the work presented in this thesis has been submitted in support of any application for any other degree of qualification to this or any other university or institute of learning.

<div align="right">

_____

Sohail Iqbal

</div>

DEDICATION

This thesis is dedicated to my Family who supported me all the way since the beginning of my studies.

Acknowledgement

I would like to thank The Allah Almighty, who blessed me with hope and courage whenever I faced difficulties during my research work.

I am extremely grateful to Dr. M Afzaal Malik who allowed me to work under his supervision. He has been very helpful and supportive. He always encouraged me and boosted my moral whenever I was depressed. Without his guidance and persistent help, this dissertation would not have been possible.

I would like to thanks honorable faculty members who served on my committee: Dr Mehmmod Anwar Khan, Dr. Syed Waheed Ul Haq ,Dr Imran Akhtar and Raja Amer Azeem for their support, guidance and useful suggestions.

My special thanks to Raja Amer Azeem who helped, supported and guided me whenever I faced difficulty in my research work.

I would like to thank my beloved parents and family, who prayed for me, their endless effort and support made it possible for me, to be, what I am today.

I would like to thanks my friend Hammad Nazeer Gilani for support, moral and memorable moments we spent during my research work.

In the end I would like to thank the entire honorable faculty of Mechanical Department of the College of Electrical and Mechanical Engineering to be so supportive.

Sohail Iqbal

March, 2012

Abstract

Micro air vehicle (MAV) is defined as unmanned air vehicles with wing to wing span of 150 mm and weight not more than 100 grams, specifications defined by American Defense Advanced Research Projects Agency (DARPA). MAV finds its applications in surveillance, rescues and other strategic military purposes. The major impediment in its adoption is range. This requires efficient aerodynamics with light weight mechanisms and least possible actuators. In this work a wing flapping mechanism is proposed. A single actuator drives both wings making the design compact. There is a provision for introducing or correcting asymmetry in flapping frequency of the two wings while keeping the amplitude fixed. Continuously varying transmission utilizing friction is used to achieve a linear change in asymmetry. The sensitivity of the frequency change mechanism can be tuned to reduce the motion and power requirements. A scaled physical prototype has been realized to verify the functionality. Loop closure and Denavit-Hartenberg approach is used to simulate the kinematics of the system. Commercial codes are used for validation and final design. A parametric study was done to establish the effect of changing parameters of this proposed mechanism. Power requirements for the scaled prototype were compared with values from software analysis. The results are in close agreement. The prototype mechanism can be used for experimental study of aerodynamics of single flapping wing or two wings flapping at different frequencies.

Table of Contents

List of Figures

List of Tables

Chapter 1: Introduction

Chapter 1: Introduction

MAV is defined as unmanned air vehicles with wing to wing span of 150 mm and weight not more than 100 grams as defined by DARPA. Small sized air vehicles with low speeds have a promising future in surveillance and rescue operations. Fixed wing, rotary wing and flapping wing are types of MAV. Flapping wing micro air vehicle is further classified into symmetric and asymmetric flapping micro air vehicles. Asymmetry in flapping is due to asymmetric amplitude and asymmetric frequency. There is very limited literature available on asymmetric flapping frequency affects. So there is a need to carry out a study on effects of asymmetric flapping frequencies and means of correcting it online if required.

A mechanism is designed which can continuously and linearly vary relative flapping frequencies. This mechanism can be design for a particular shift in frequency with a desired sensitivity. Conversely a desired asymmetry in flapping frequencies can also be achieved with a single actuator with precision. Continuous variable transmission concept is chosen as it provides continuous variable speed ratios with the help of single actuator. A mechanism is designed which is capable of generating variable flapping frequencies using single actuator. To design a flapping mechanism for micro air vehicle, a detailed literature survey of micro air vehicles and the already designed mechanisms is carried out. To accomplish the task of design and analysis of mechanism detailed survey is carried out on current research on micro air vehicles and set of analysis particularly kinematic and dynamics.

1.1 Motivation

Study of flapping mechanism is an important part of micro air vehicle research. Good design and better understanding of kinematic and dynamic effects can improve the flying capabilities of MAV. During flight any abnormality like dislocation of joint or link can lead to an abrupt change in frequency of wings causing it to crash, a mechanism which can adjust a drastic change in frequency will improve stability and flight safety. It is very important to study the effects caused by asymmetric flapping frequencies. To study the effects of asymmetric flapping frequencies a mechanism is required, that is why a mechanism which can produce asymmetric flapping frequencies is designed. A mechanism which cannot only produce asymmetric flapping frequencies but capable of adjusting frequencies will definitely improve flying characteristics of flapping vehicle.

1.2 Literature Review

A micro air vehicle is a sub type of unmanned air vehicle that has small size and weight. The word Micro air vehicle was first called by a Washington Post [1]. In early 90, a suitable solution to the missions of reconnaissance in constrained environments seemed to be Micro Air Vehicle. DARPA took initiative and started conducting workshops on MAVs. A grand project was started whose mandate was to develop high autonomy unmanned, light weight, low cost, maximum dimension of 15 cm aircraft. In aerodynamics context such a small size aircraft could be placed in air flow range of low Reynolds number flows, between 10^2 to 10^4. Research was started and numbers of prototypes were developed on concept of fixed and rotary wings. Research on insects and birds gave rise to an idea of flapping wing. MAV applications are both civil and military purposes and working in those areas and environment which are unreachable by traditional vehicles.

1.2.1 Classification

MAVs are classified into three types based on its flying mechanism

1. Fixed wing
2. Rotary wing
3. Flapping wing

1.2.1.1 Fixed Wing

They are similar to aircrafts, speeds are high and they can cover longer distances however cannot maneuver much effectively.

1.2.1.2 Rotary Wing

They are similar to helicopters, sometimes called choppers, their maneuvering capabilities are better than fixed wing MAV and they can be launched and landed in short time and at short distances.

1.2.1.3 Flapping Wing

Flapping wing inspiration came from nature. These types are superior to both fixed and rotary wing both in maneuvering and control at high altitudes. A

flapping wing can generate thrust and lift at same time, flight control is better and it is more efficient than the other two.

In MAV research, insects and birds are being studied in detail, their biological systems, that is aerodynamics, control and sensing are main areas of interest. Symposiums bringing together biologists and aerial robot cists have been held in 2007[2], and some books have recently been published on this topic.

Engineers succeeded in developing a DelFly Micro air vehicle [3] as shown in figure 1-1. Its 3rd version of DelFly, remote-controlled with spying cameras, just 3 grams, 10 cm wide, 1 gram battery. As a result of set of analysis done on DelFly it can be deduced that if asymmetry is introduced in the MAV it will cause a roll in the MAV. Research on DelFly NaNo is under process now a day.
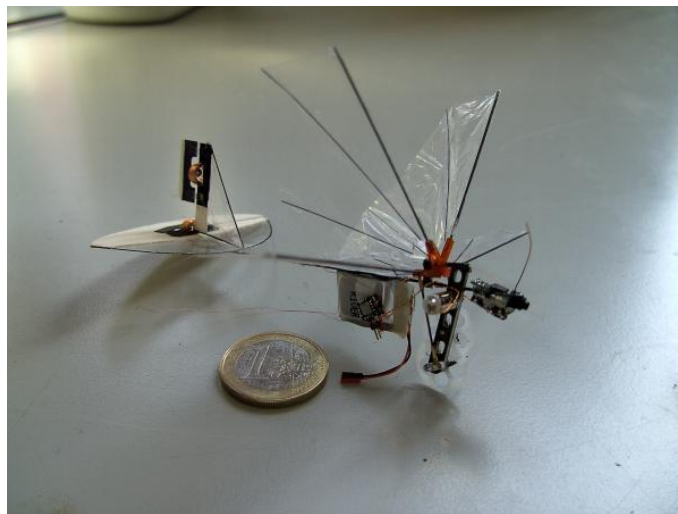
Figure 1-1 The DelFly Micro [3]

Flapping wing mechanism can be classified as symmetrical flap and asymmetrical flap. The mechanism with **symmetrical** flap produces no lag; time delay in flap; difference in flap neither frequency nor amplitude between the wings. In this type both wings flap with same frequency, it is unfavorable in turning.

Asymmetry in flapping can be classified as following:

1. Different amplitude of the wings with the same frequency.
2. Different frequency of the wings with same amplitude.
3. Different frequency and amplitude.

4

MAV research can be done in two ways; either to observe birds flying or to perform wing analysis [4]. The literature mainly focuses on asymmetry for controlling the flight.

Currently existing mechanism study is very important for designing a new type of mechanism. Now a day's many unmanned air vehicle (UAV) and MAV are in research and development phase. UAV is an air vehicles remotely controlled by a navigator or pilot. Some UAV close to the limits defined by DARPA are Dragon Eye [5], Mite 2 [6] and Black Widow [7].

Mcintosh et al [8] created a flapping mechanism which can change pitch angle as shown in figure 1-2. This type uses a single actuator for both flapping and pitching mechanisms. Gear assemblies and connecting rods are used to produce plunging motions, pin and follower assembly is used for pitching. This type varies pitch during flight.

Figure 1-2 McIntosh flapping wing mechanism [8]

Based on research on insects the Microbot developed by Pornsin-Sirirak [9] as shown in figure 1-3, is a MAV with MEMS based membrane wings, titanium-alloy (Ti6Al-4V) wings and parylene for the skin. This design is powered by a DC motor with 22:1 gearing reduction and flap at 30 Hz.
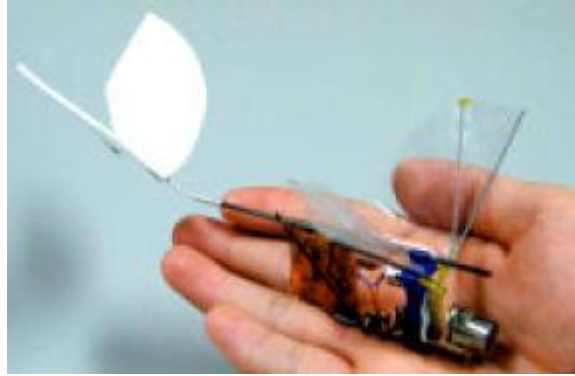
Figure 1-3 Microbot [9]

Microbot Transmission System and Fabricated UAV [10] flapping wing flight is more efficient than fixed wing because a bird can maneuver in so many different ways which is not achievable by fixed wing. They are more stable in gusty environment, more resistant to stalling and are smoother in flight.

1.3 Existing Mechanisms for Wing Flapping

Some mechanisms have been built where rigid wings are flapped and experimented; there is dynamic pitch and amplitude control [11]. These experiments have been conducted in water, and the flapping frequencies are very low, allowing the motors which control both degrees of freedom to work together more easily. Currently, the only mechanisms which alter pitch do so in direct drive forms, meaning the rates of pitch change and deflection of the pitch angles are constant for a given frequency [11].

Gautam Jadhav designed a mechanism which can flap and pitch [12]. A single electric motor was used which flapped a flexible wings and the aerodynamic forces generated by flexible membrane wings were measured using a two degree of freedom force balance. Different set of wings were made mainly differing in flexibility and thirteen case studies were conducted. These cases include zero velocity free stream conditions with different flapping frequencies. High speed videos were made and the images from the video were also correlated with cycle averaged aerodynamic forces produced by the mechanism. Based on these experiments he gave useful suggested regarding the behavior of flexible flapping wings that should aid in future of flapping wing mechanisms. Figure 1-4 shows the mechanism of reference [12].

6

Figure 1-4 Isometric view of mechanism [12]

In research being done at Madras Institute of Technology different mechanisms have been proposed focusing on angle of flap and flapping frequency as shown in figure 1-5.
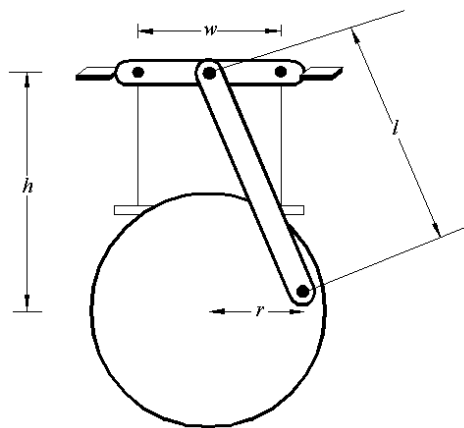
Figure 1-5 Generalized mechanism [13]

This mechanism shown in figure 1-5 can produce symmetrical and asymmetrical flap in two different design concepts. Mathematical model for this mechanism was made where key parameters can be easily changed and graphed.

A sliding link mechanism has a crank and a motor as shown in the figure 1-6. A connecting rod connects crank and tube. The tube has holes for sliding link. The sliding links are hinged at two different locations at proper lengths. Height of hinge with reference to base and distance between them is also fixed. As crank rotates links slide into tube and starts flapping.
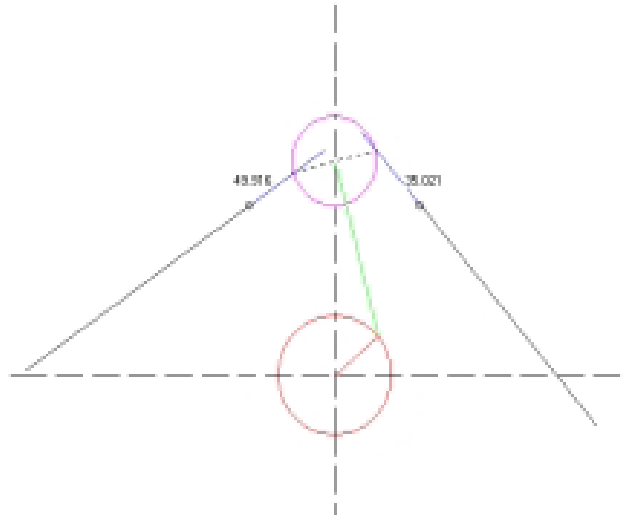
Figure 1-6 Sliding link mechanism [13]

A moveable hinge mechanism has a crank and a motor as shown in the figure 1-7. A connecting rod connects crank and links using fasteners, links are connected to base by flexible struts.
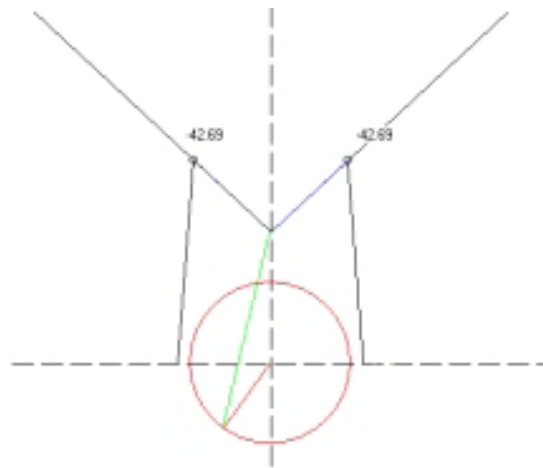
Figure 1-7 Moveable hinge mechanism [13]

A light weight butterfly type ornithopter (BTO) is made to investigate a butterfly flight as shown in figure 1-8(a). Its weight is 0.4 gm, wing span is 140 mm and flapping frequency is 10 Hz with flying forward capability. A cyclic change of angle of attack, having appropriate center of gravity can produce upward aerodynamic force. Crank and linkages of BTO are shown in figure 1-8(b) and sample of butterfly is shown in figure 1-8(c). The airflow was visualized around the BTO both in tethered flight and in free flight and concluded that free body motion caused a stable attachment of leading edge vortex and helped the wings smooth upstroke, which was not found in tethered flight [14].

8
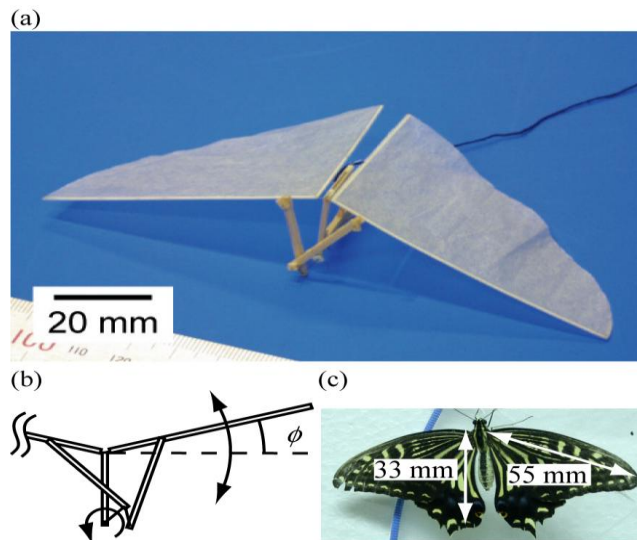
Figure 1-8 (a) A photograph of BTO (b) Crank and linkages of BTO (c) A sample of a butterfly [14]

An ornithopter which can mimic a humming bird is designed. The hummingbird simultaneously feathers or rotates its wings in order to attain its hovering ability [15]. To make such a mechanism different types of gears, actuators, joints and structural supports were used. A biological inspired robot is currently a new subject of study and research. Biological robots are proved to be more efficient than traditional types. Various robots have been designed so for to mimic the behavior of cockroaches, snakes, lizards, and even birds [15].

In 2002 engineers at Chalmers University of Technology in Sweden [16], constructed a flapping wing robot that was capable of learning flight techniques. The ornithopter was driven by machine learning software known as a steady state linear evolutionary algorithm. This software was able to "evolve" in response to feedback on how well it performs at a given task. As a result, this mechanism evolved the ability for horizontal movement and maximum sustained lift force. Fixed wings depend on forward velocity in order to generate maneuvering forces; flapping wings can produce large maneuvering forces at any given time [16].

Manuel Naef adopted a four wing concept to design a flapping mechanism. His goal of research was to design a MAV than can hover. Two actuators were less to control roll, pitch rate and height. Keeping in view design limitations best approach was to use

another pair of wings, actuated by a motor. Using four wings allows dividing the mechanism into two identical subsystems, each comprising of two wings capable of controlling the roll and pitch rate mandatory for hovering. By using four wings concept possibility to control the Yaw rate increases. On the basis of the angular speed it may be possible to obtain a resulting force that would induce a yaw rate. Subsystem consisted of two wings with independent actuation chain. Each subsystem flap horizontally. Flapping is taking place in x-y plane while z axis is at center of rotation. The two subsystems are shown in the figure 1-9. The subsystems were rotated 90° around the z axis; an offset of one chord length of the wing in vertical direction is given between two flapping planes. The offset is given to give room for flapping. In this case each wing can be actuated separately [17].
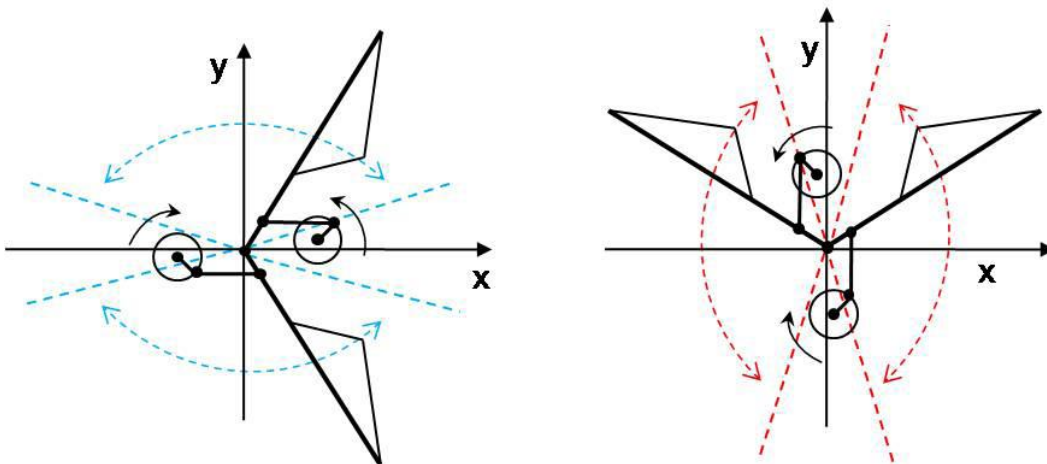
Figure 1-9 The two sub mechanisms are identical but rotated by 90 around the z-axis [17]

Mechanism was flapped by a continuous 360° rotation from the actuator, which was transmitted to wing by a link. The motors chosen are Micro DC Motors of 6mm diameter and 15mm length from Precision Micro drives (Model 106-002). Wing was manufactured by carbon rod to which a plastic foil was attached such that the wing can pitch freely without resistance [17].

Optimization of flapping wing trajectory was explored using an experimental setup. A three degree of freedom mechanism was used for experimentation of a scaled up wing. Load cells were used for measuring forces and wing path was optimized to maximize

average force. The mechanism design, control, and instrumentation, and the optimization approach were discussed [18].

A mechanism for micro air vehicle was designed which can store a percentage of kinetic energy during flapping in the form of elastic potential energy. Dynamic model was established to optimize the parameters for energy storage [19].

A mechanism to mimic insect wing motion was designed and fabricated. Twisting of wing and out of plane flapping was the mandate. The mechanism designed is five bar mechanism having single degree of freedom. To generate required motion mechanism parameters were optimized. To verify the practical feasibility a scaled model of mechanism was fabricated with flexible wing [20].

Insect flights and flapping wing MAVs have become a popular area for research in the last few years [21]-[27]. Wotton has studied the acrobatics of flight and mechanics structure of different insect's wings and enlightened the remarkable features of flight acrobatics [28]. Finite element methodology was used by Smith. He presented the effects of mechanization of flapping wing flight through moth wing modeling [29].

A four bar linkage flapping wing MAV was built by Lan Liu capable of flying as shown in figure 1-10. MAV crashed due to wrong symmetry of wings, so to improve its efficiency design optimization was studied [30].
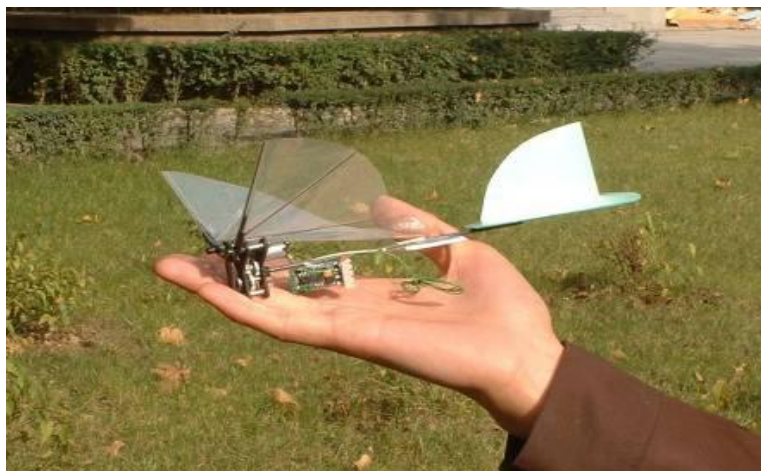

Figure 1-10 Flapping wing MAV by Lan Liu [30]

1.4 Objective

Objective of research are

a. To design a mechanism capable of producing or correcting asymmetry in flapping frequencies so that the effects of asymmetry can be studied.

b. To carry out a kinematic, dynamic and parametric study of designed mechanism.

c. To fabricate a prototype to verify the functionality of design using it as a test bench to measure power requirements of flap for different wings.

1.5 Contribution

MAV is a very emerging area in research now days because of its applications in warfare and rescue missions. Due to the state of the art technology and resources remarkable work and achievements has been achieved but a lot of research has to be discovered yet specially in the field of asymmetric flapping frequencies. In this research a mechanism that can vary frequency has been designed and expected results are achieved. A new design concept has been introduced, with a design concept of frictional continuous variable transmission. The goal of generating variable flapping frequencies has been accomplished using single actuator. A prototype has been manufactured which proves the functionality of design concept and capable of measuring flapping powers for different wings.

1.6 Summary

The report has following structure. In chapter 2 designing of mechanism are explained with specifications. Chapter 3 contains mathematical modeling using loop closure equations and Denavit-Hartenberg approach. In this chapter two more mechanism are modeled to extract input variables for the designed mechanism and results validated with commercial codes. In chapter 4 fabricated prototype is explained and experimentation regarding power requirements of flap are explained. In chapter 5 kinematic and dynamic results are discussed. At the end conclusion summarizes the results of chapter 4 and 5 followed by recommendations for future research.

Chapter 2: System Description

Chapter 2: System Description

We need to design a mechanism which is capable of generating asymmetric flapping frequencies. Asymmetric frequencies can also be achieved with different design concepts. Two actuators can be used to vary frequency but the limitation is to use single actuator because two motors will increase weight and power requirements for which we have to use high power battery, which will ultimately increase battery size and weight, as we have design limitations for size and weight we cannot use two actuators and large size heavy weight battery so a new concept is used which can vary frequency successfully with single actuator. In this design one actuator is driving the mechanism and second actuator is changing the longitudinal position of disk, second actuator is just operating for a fraction of time and can be very small in size, power requirement for whole mechanism is reduced. Gears can also be used to vary frequency but gears can just produce vary single frequency ratio, for different frequency ratios new set of gears are to be used, then changing of drive from one set to other is complex and a heavy arrangement. The best suited concept is frictional continuous variable transmission.

Specifications of system are given in table below.

Table 2-1 System specifications

s/no	Component/Link	Link Length (mm)	Thickness(mm)	Radius (mm)
1	Rotating Disk	___	10	30
2	Wheel	___	10	12.5
3	Connection rod	42	___	5
4	Wing	36	1	___

Mechanism of Micro air vehicle constitutes of rigid links and joints driven by an actuator. Revolute and spherical joints are used to connect linkages. Revolute joint is a joint which can produce rotational motion in one dimension and spherical joint is a joint which can produce rotational motion in three dimensions. Revolute joint is also called pin joint and spherical joint is also called ball joint. System consists of crank, connecting rod, rocker, and driving plate. A

motor has been connected to the drive shaft of the main disk, which further drives the whole mechanism to give required motion. The central flapping drive motor can be placed at any longitudinal position to adjust the center of gravity of the vehicle. A second actuator is required to position the disk. This arrangement requires less frequent input energy. This shifting would also introduce a slight lateral shift in the center of gravity resulting in a moment assisting the moment caused by frequency shift.

As the distance of wheel changes form the center of disk angular velocity changes accordingly, resulting in a differential shift in the flapping frequency of wings. Figure 2-1 shows Pro Engineer model and schematic diagram of proposed mechanism.
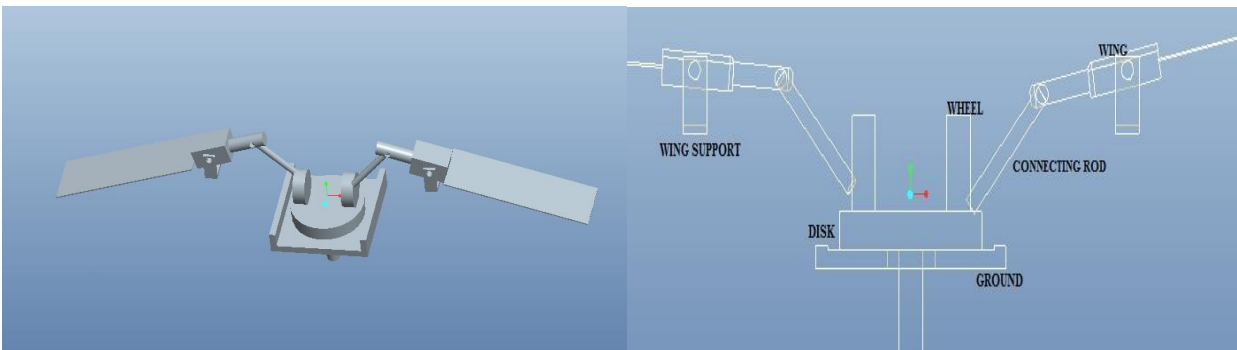

Figure 2-1 (a) Designed flapping wing mechanism (b) Schematic diagram of mechanism

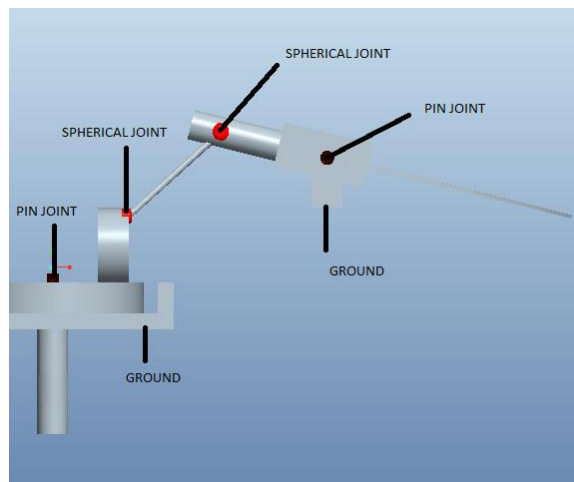Figure 2-2 shows joints used in proposed mechanism.

Figure 2-2 Flapping wing mechanism joints

Details of mechanism are given below.
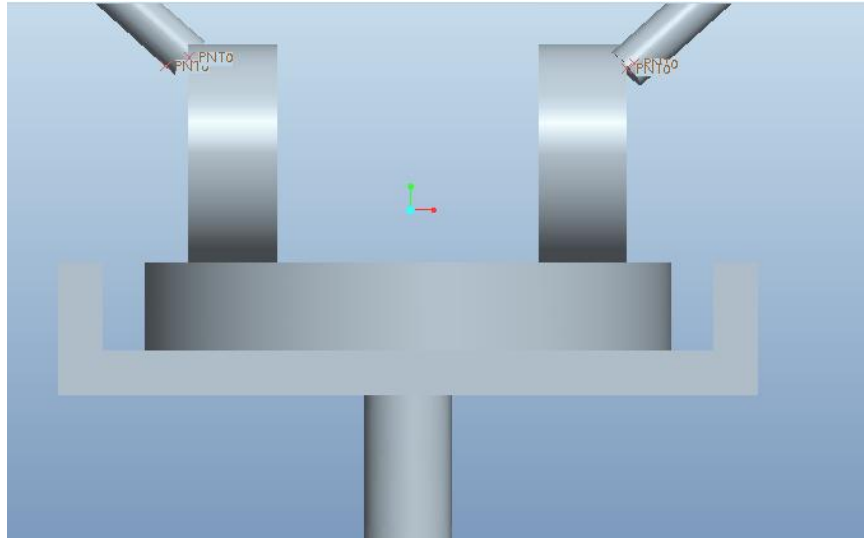
2.1 Rotating Disk

Figure 2-3 Rotating disk

A rotating disk can rotate and its translation is restricted with ground reference as shown in figure 2-3. It can rotate with different RPM as required for motion/analysis.

2.2 Rotating Wheels

Connection between rotating disk and rotating wheels is a frictional contact. This is between surfaces of rotating wheel and rotating disk. In this contact friction is created between these for transmission. A wheel rides upon the surface of a rotating disk; the wheel may be slid along to contact the disk at different distances from its center [31] as shown in figure 2-4. The two wheels axes are coincident for smooth transmission. Transmission of motion depends on the

1. wheels radius
2. rotating disk radius
3. motor RPM
4. frictional contact surfaces
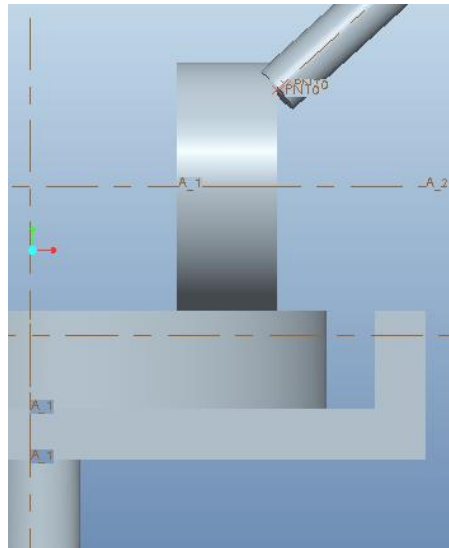5. distance of rotating wheel from axis of rotation of drive shaft

Figure 2-4 Rotating wheel

2.3 Connecting Rod

Connecting rod has to convert rotating motion into up and down motion of flapping wing mechanism as shown in figure 2-5. Connecting Rod is connected to rotating wheel through spherical ball joint on one side and wing on other side. Spherical joints is used here because a joint is needed in which translation is fixed while rotation is free. A spherical joint is a six degree of freedom joint giving rotations in three directions. It generates a three axis rotation function. A spherical joint can also be said a combination of three revolute joints.
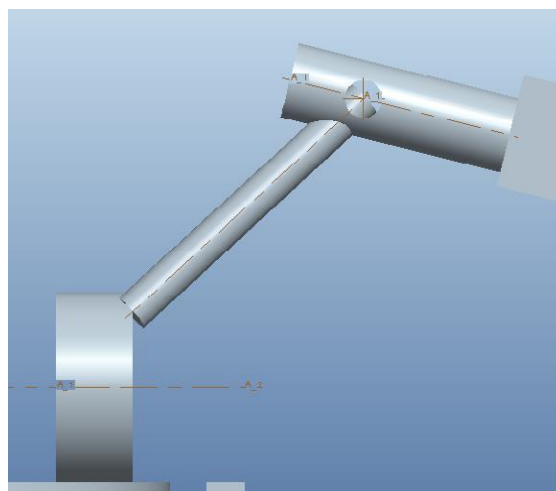

Figure 2-5 Connecting rod

2.4 Wing Connections

Wing is connected to wing support through revolute joint so that it can flap up and down easily as shown in figure 2-6. A single-axis rotation function is being used in wing support, so that it can flap.
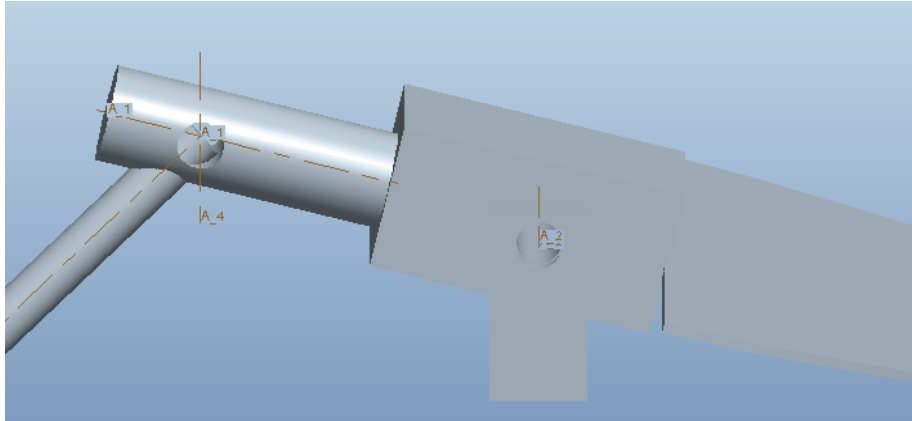

Figure 2-6 Wing connection

2.5 Continuous Variable Transmission

A frictional continuous variable transmission is used for motion transfer from disk to wheel. Wheel rides on the disk, as disk rotates due to frictional contact wheel also rotates. In this way friction transfer motion between two bodies at varying distance points. Rotating disk and wheel have rough surfaces. A wheel rides upon the surface of a rotating disk; the wheel may be slid along to contact the disk at different distances from its center.

2.6 Material Properties

Aluminum and mild steel is used to fabricate the mechanism. Disk is fabricated with mild steel and wheels are made up of aluminum. Aluminum is used to reduce weight of mechanism and mild steel is used where high strength is required [32].

Chapter 3: Mathematical Modeling of Flapping wing mechanism of MAV

Chapter 3: Mathematical Modeling of Flapping Wing Mechanism of MAV

3.1 Introduction

Figure 3-1 Designed mechanism

Mechanism kinematics is modeled using two approaches; one is loop closure approach and second is Denavit-Hartenberg approach. First technique is based absolute coordinate system and second one on relative coordinate system.

The designed mechanism is shown in figure 3-1. In kinematic analysis of mechanism first step is to choose a coordinate system so that position of linkages can be uniquely defined. Different coordinates can be used to describe multi-body system.

Choice of coordinate system whether dependent or independent describing position, velocity or acceleration varies from problem to problem. Number of independent coordinates and number of degrees of freedom are same. Dependent coordinates are easier to understand and solve. Three coordinate systems are defined for designed mechanism as shown in the figure 3-2.
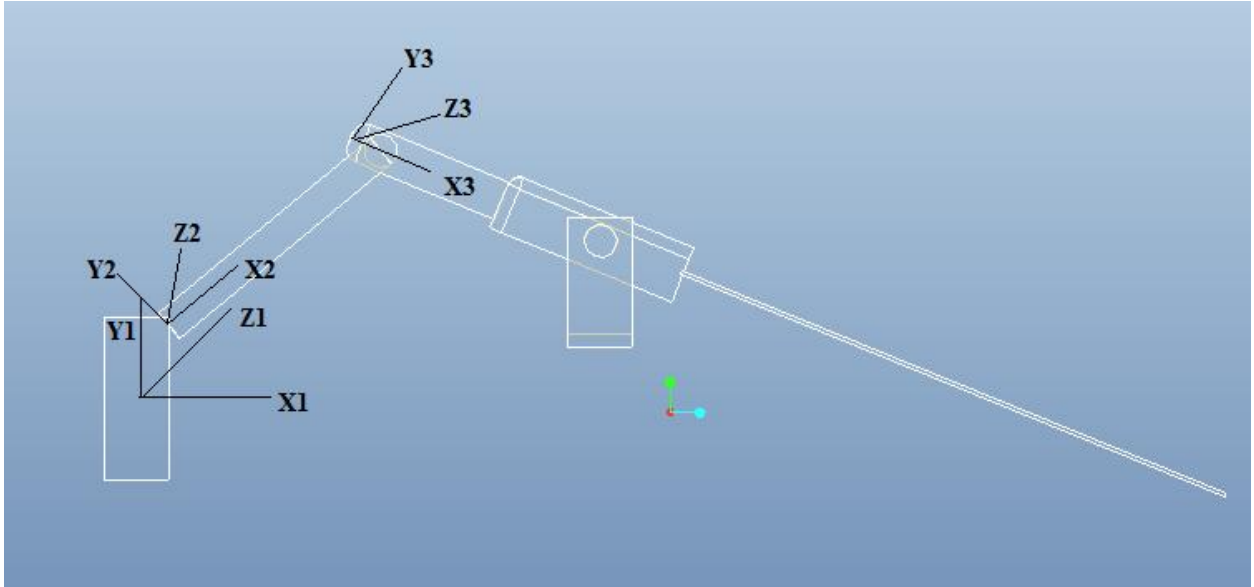
Figure 3-2 Coordinates of mechanism

Link lengths are selected by Grashof condition. Grashof condition states that for a four bar planer mechanism sum of smallest and longest link length should not be greater than the sum of other two link lengths for complete rotation of smallest link. Two link lengths were selected and the other two were found using Grashof condition. Link lengths were adjusted for the desired motion of flap. Link that can fully rotate is also called crank. Output link is also called rocker and the link connecting crank and rocker is also called coupler. As the mechanism is 3D so for Grashof condition we will consider projected lengths. The designed mechanism is 1 degree of freedom system.

3.2 Loop Closure Approach

Basic constraint equations for the mechanism are

$$(x_2-x_1)^2 +(y_2-y_1)^2+ (z_2-z_1)^2 = L^2_3 \tag{3.1}$$

$$(x_2-x_3)^2 + (y_2-y_3)^2 = L_4^2 \tag{3.2}$$

L_3 and L_4 are the link lengths as shown in the figure 3-1.

3.2.1 Position

Rewriting equations (3.1) and (3.2) gives

$$x_2^2 - 2x_1x_2 +y_2^2 - 2y_1y_2 = A \tag{3.3}$$

21

$$x_2{}^2 - 2x_2x_3 + y_2{}^2 - 2y_2y_3 = B \qquad\qquad (3.4)$$

Where,

$$A = L_3{}^2 - x_1{}^2 - y_1{}^2 - z_2{}^2 - z_1{}^2 + 2z_1z_2$$

$$B = L_4{}^2 - x_3{}^2 - y_3{}^2$$

$$C = \frac{A-B}{2(X_{3-}X_{2)}}$$

$$D = \frac{y_2(y_3-y_1)}{x_{3-}x_1}$$

Solving equations (3.3) and (3.4) gives,

$$y_2 = \frac{-(-2CD+2Dx_1-2y_1)\pm\sqrt{(-2CD+2Dx_1-2y_1)^2-4(D^2+1)(C^2-2Cx_1-A)}}{2(D^2+1)} \quad (3.5)$$

$$x_2 = C - Dy_2 \qquad\qquad (3.6)$$

Solving above equations give two values of y_2 and x_2, y_2 and x_2 are positions at x and y axis respectively of L_4, as the link is revolute jointed there is no movement in z axis. L_4 is also called flap link. Based on system requirement and relative constraints we choose one value of y_2 and x_2.

3.2.2 Velocity

Velocity equations can be derived from position equations by differentiating them with respect to time.

Differentiation of variable A gives,

$$\frac{dA}{dt} = -2y_1\frac{dy_1}{dt} - 2z_1\frac{dz_1}{dt}$$

Differentiation of variable B gives,

$$\frac{dB}{dt} = 0$$

Differentiation of variable C gives,

$$\frac{dC}{dt} = [-y_1 \frac{dy_1}{dt} - z_1 \frac{dz_1}{dt} + z_2 \frac{dz_1}{dt}]/ (x_3 - x_1)$$

Differentiation of variable D gives,

$$\frac{dD}{dt} = \frac{-1}{x_3 - x_1} \frac{dy_1}{dt}$$

E=CD

Differentiation of variable E gives,

$$\frac{dE}{dt} = C \frac{dD}{dt} + D \frac{dC}{dt}$$

$$\frac{dy_2}{dt} = -2D y_2^2 \frac{dD}{dt} + 2y_2 \frac{dE}{dt} - 2x_1 y_2 \frac{dD}{dt} + 2y_2 \frac{dy_1}{dt} - 2C \frac{dC}{dt} + 2x_1 \frac{dC}{dt} + \frac{dA}{dt} \quad (3.7)$$

$$\frac{dx_2}{dt} = \frac{dC}{dt} - (D \frac{dy_2}{dt} + y_2 \frac{dD}{dt}) \quad (3.8)$$

3.2.3 Acceleration

Acceleration equations can be derived from velocity equations by differentiating them with respect to time.

Differentiation of variable $\frac{dA}{dt}$ gives,

$$\frac{d^2 A}{dt^2} = -2[y_1 \frac{d^2 y_1}{dt^2} + (\frac{dy_1}{dt})^2] - 2[z_1 \frac{d^2 z_1}{dt^2} + (\frac{dz_1}{dt})^2]$$

Differentiation of variable $\frac{dB}{dt}$ gives,

$$\frac{d^2 B}{dt^2} = 0$$

Differentiation of variable $\frac{dC}{dt}$ gives,

23

$$\frac{d^2C}{dt^2} = [-\{y_1 \frac{d^2y_1}{dt^2} + (\frac{dy_1}{dt})^2\} - [\{\frac{d^2z_1}{dt^2} + (\frac{dz_1}{dt})^2\}]/ (x_{3-}x_1)$$

Differentiation of variable $\frac{dD}{dt}$ gives,

$$\frac{d^2D}{dt^2} = - (\frac{d^2y_1}{dt^2})/ (x_{3-}x_1)$$

Differentiation of variable $\frac{dE}{dt}$ gives,

$$\frac{d^2E}{dt^2} = C\frac{d^2D}{dt^2} + \frac{dC}{dt}\frac{dD}{dt} + D\frac{d^2C}{dt^2} + \frac{dC}{dt}\frac{dD}{dt}$$

Acceleration equations are:

$$\frac{d^2y_2}{dt^2} = -2Dy_2^2\frac{d^2D}{dt^2} - 8Dy_2\frac{dD}{dt}\frac{dy_2}{dt} - 2y_2^2(\frac{dD}{dt})^2 - 2D^2 \ (\frac{dy_2}{dt})^2 + 4\frac{dE}{dt}\frac{dy_2}{dt} + 2y_2\frac{d^2E}{dt^2} -$$

$$4x_1\frac{dD}{dt}\frac{dy_2}{dt} - 2y_2x_1\frac{d^2D}{dt^2} + 2\frac{dy_2}{dt}\frac{dy_1}{dt} + 2y_2\frac{d^2y_1}{dt^2} + 2\frac{dy_1}{dt}\frac{dy_2}{dt} - 2C\frac{d^2C}{dt^2} \ 2(\frac{dD}{dt})^2 + 2x_1\frac{d^2C}{dt^2}$$

$$+\frac{d^2A}{dt^2} - 2(\frac{dy_2}{dt})^2 \qquad\qquad\qquad (3.9)$$

$$\frac{d^2x_2}{dt^2} = \frac{d^2C}{dt^2} - \left(D\frac{d^2y_2}{dt^2} + \frac{dy_2}{dt}\frac{dD}{dt}\right) - [y^2\frac{d^2D}{dt^2} + \frac{dD}{dt}\frac{dy_2}{dt}] \qquad\qquad (3.10)$$

3.3 Denavit-Hartenberg Approach

DH approach is carried out to study kinematics of designed mechanism. Loop closure approach is based on absolute coordinate system, while DH approach is based on relative coordinate system. Kinematic analysis by loop closure equation is already explained. DH approach is representation of homogenous transformation as the product of four basic parameters. DH approach has been applied to the mechanism with details given below. Let us consider a link as shown in the figure 3-3. To describe the position of a link with respect to its neighbor link we define a frame attached to that link and frames are numbered in accordance with link number.
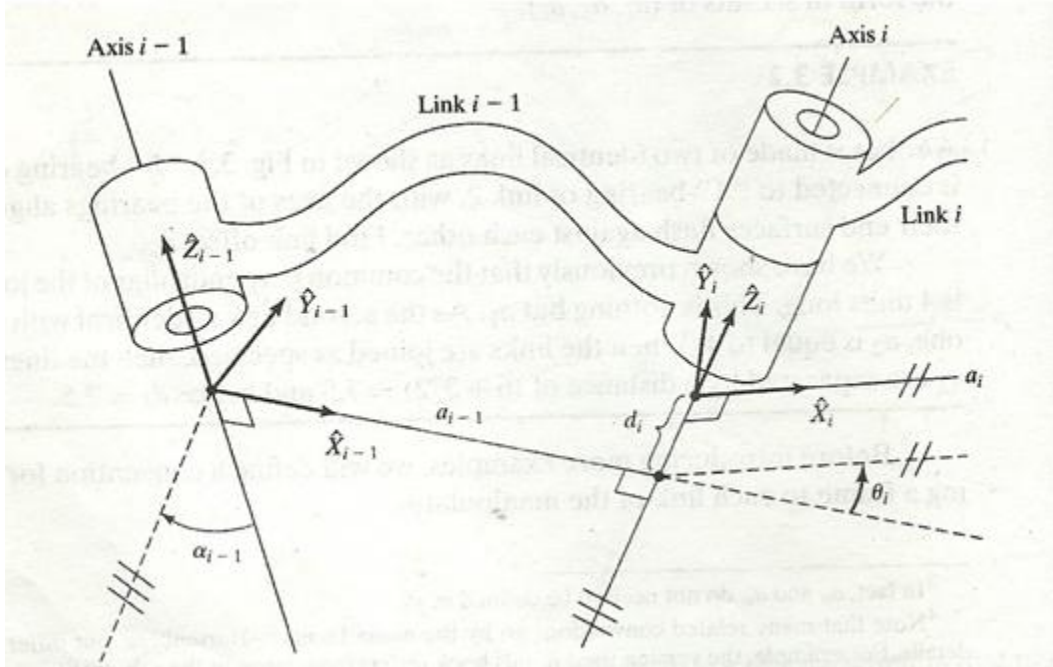
Figure 3-3 Rigid link [32]

DH parameters are

α_i = the angle from Z_i to Z_{i+1} measured about X_i

a_i = the angle from Z_i to Z_{i+1} measured about X_i

d_i = the distance from X_{i-1} to X_i measured along Z_i

θ_i = the angle from X_{i-1} to X_i measured about Z_i

Transformation matrix used in Denavit-Hartenberg Notations is:-

$$
{}^{i-1}_{i}T = \begin{bmatrix}
\cos\theta i & -\sin\theta i & 0 & ai-1 \\
\sin\theta i\, cos\alpha i-1 & \cos\theta i\, cos\alpha i-1 & -sin\alpha i-1 & -sin\alpha i-1di \\
\sin\theta i\, cos\alpha i-1 & \cos\theta i\, sin\alpha i-1 & cos\alpha i-1 & cos\alpha i-1di \\
0 & 0 & 0 & 1
\end{bmatrix}
$$

First three columns are of rotation transformations and last column is of linear transformation. Finding the position of link *i* with respect to link *i-1* is forward kinematics and finding the position of link *i-1* with respect to link *i* is inverse kinematics.

For the designed mechanism we define link lengths, distances and link angles as shown in the figure 3-4. Four body coordinate systems are defined for designed mechanism as shown in the figure 3-5. First DH table is made and respective transformation matrices are written followed by the overall transformation matrix.
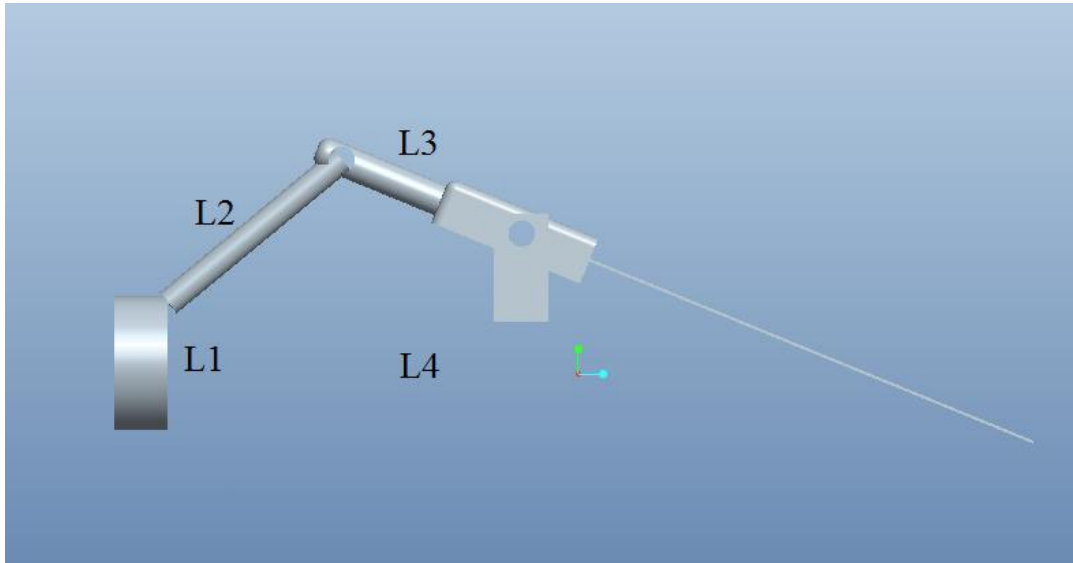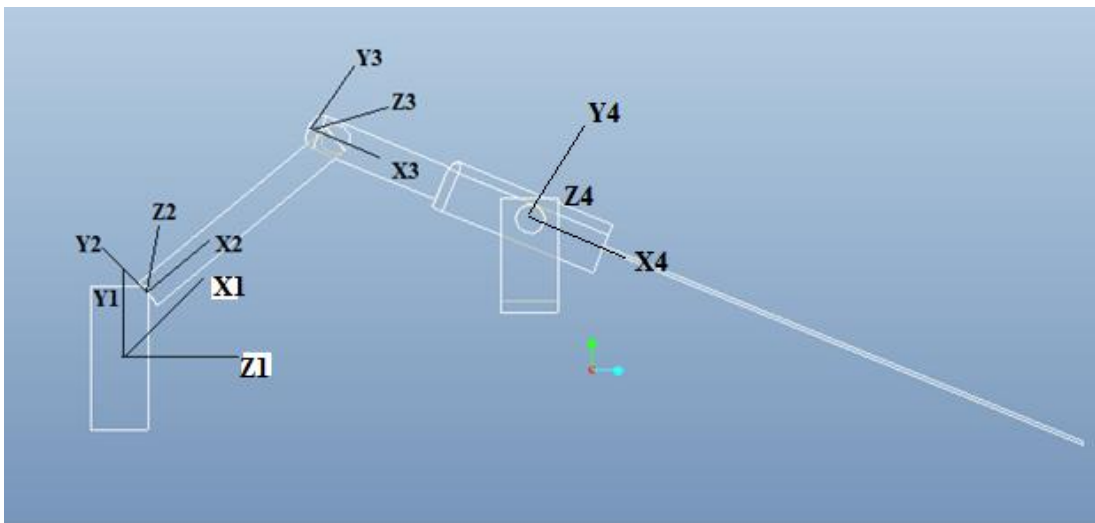

Figure 3-4 Designed mechanism

Figure 3-5 Designed mechanism

3.3.1 DH Table for Designed Mechanism

DH table of designed mechanism along with parameters is table 3-1.

Table 3-1 DH table for designed mechanism

i	α_{i-1}	a_{i-1}	d_i	θ_i
1	0	0	0	θ1
2	-90	L1	0	θ2
3	90	0	0	θ3
4	0	0	0	θ4
5	-90	L2	0	θ5
6	90	0	0	θ6
7	0	0	0	θ7
8	0	L3	0	θ8

3.3.2 DH Transformations

Transformation matrices are

$$
{}^{0}_{1}T = \begin{bmatrix} \cos\theta1 & -\sin\theta1 & 0 & 0 \\ \sin\theta1 & \cos\theta1 & 0 & 0 \\ 0 & 0 & 1 & 0 \\ 0 & 0 & 0 & 1 \end{bmatrix}
$$

$$
{}^{1}_{2}T = \begin{bmatrix} \cos\theta2 & -\sin\theta2 & 0 & L1 \\ 0 & 0 & 1 & 0 \\ -\sin\theta2 & -\cos\theta2 & 0 & 0 \\ 0 & 0 & 0 & 1 \end{bmatrix}
$$

$$
{}^2_3T = \begin{bmatrix} \cos\theta 3 & -\sin\theta 3 & 0 & 0 \\ 0 & 0 & -1 & 0 \\ \sin\theta 3 & \cos\theta 3 & 0 & 0 \\ 0 & 0 & 0 & 1 \end{bmatrix}
$$

$$
{}^3_4T = \begin{bmatrix} \cos\theta 4 & -\sin\theta 4 & 0 & 0 \\ \sin\theta 4 & \cos\theta 4 & 0 & 0 \\ 0 & 0 & 1 & 0 \\ 0 & 0 & 0 & 1 \end{bmatrix}
$$

$$
{}^4_5T = \begin{bmatrix} \cos\theta 5 & -\sin\theta 5 & 0 & L2 \\ 0 & 0 & 1 & 0 \\ -\sin\theta 5 & -\cos\theta 5 & 0 & 0 \\ 0 & 0 & 0 & 1 \end{bmatrix}
$$

$$
{}^5_6T = \begin{bmatrix} \cos\theta 6 & -\sin\theta 6 & 0 & 0 \\ 0 & 0 & -1 & 0 \\ \sin\theta 6 & \cos\theta 6 & 0 & 0 \\ 0 & 0 & 0 & 1 \end{bmatrix}
$$

$$
{}^6_7T = \begin{bmatrix} \cos\theta 7 & -\sin\theta 7 & 0 & 0 \\ \sin\theta 7 & \cos\theta 7 & 0 & 0 \\ 0 & 0 & 1 & 0 \\ 0 & 0 & 0 & 1 \end{bmatrix}
$$

$$
{}^7_8T = \begin{bmatrix} \cos\theta 8 & -\sin\theta 8 & 0 & L3 \\ \sin\theta 8 & \cos\theta 8 & 0 & 0 \\ 0 & 0 & 1 & 0 \\ 0 & 0 & 0 & 1 \end{bmatrix}
$$

Rotational and translational transformation of elements can be found out by multiplication of these transformation matrices. Overall transformation matrix is ${}^0_8T$. L1, L2, L3 are link lengths and θ1 to θ8 are joint angles. To find angles two more mechanisms are modeled and solved. For each degree change in input there is a unique transformation matrix i.e. for one complete revolution of crank there will be 360 matrices. The designed flapping wing mechanism is a four bar 3 dimensional mechanisms. For solving this mechanism two more mechanisms are designed and analyzed using DH approach and software. A four bar crank rocker mechanism and three link 3 D mechanism are designed; by inverse kinematics approach we can find unknown angles.

3.4 Crank Rocker Mechanism

A planar four bar mechanism is designed and solved using DH approach to find variable angles. Same mechanism is solved using software as shown in the figure 3-6.
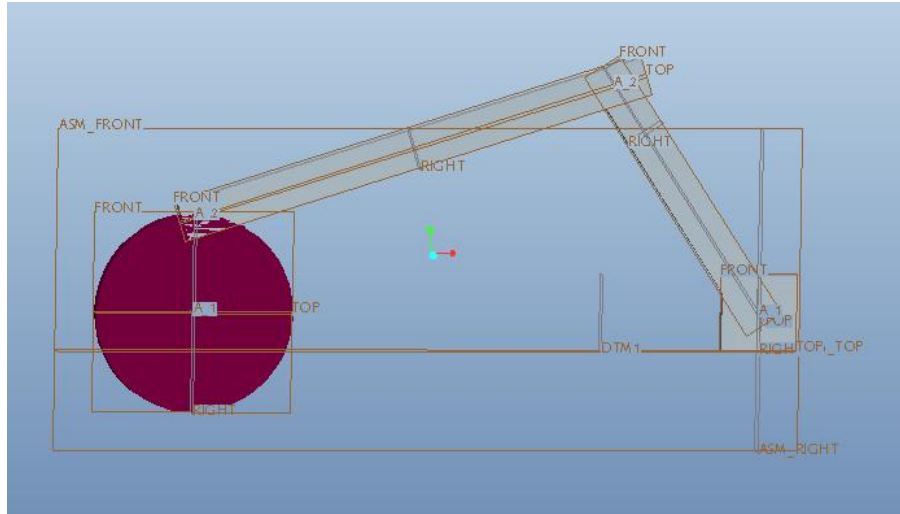

Figure 3-6 Crank rocker mechanism

3.4.1 DH Table

DH table for crank rocker mechanism is given in table 3-2.

Table 3-2 DH table for crank rocker mechanism

i	α_{i-1}	a_{i-1}	d_i	θ_i
1	0	0	0	θ_1
2	0	L1	0	θ_2
3	0	L2	0	θ_3
4	0	L3	0	θ_4

3.4.2 Transformation Matrices

Transformation matrices for four bar mechanism are;

$$
{}^{0}_{1}T = \begin{bmatrix} \cos\theta 1 & -\sin\theta 1 & 0 & 0 \\ \sin\theta 1 & \cos\theta 1 & 0 & 0 \\ 0 & 0 & 1 & 0 \\ 0 & 0 & 0 & 1 \end{bmatrix}
$$

$$
{}^{1}_{2}T = \begin{bmatrix} \cos\theta 2 & -\sin\theta 2 & 0 & L1 \\ \sin\theta 2 & \cos\theta 2 & 0 & 0 \\ 0 & 0 & 1 & 0 \\ 0 & 0 & 0 & 1 \end{bmatrix}
$$

$$
{}^{2}_{3}T = \begin{bmatrix} \cos\theta 3 & -\sin\theta 3 & 0 & L2 \\ \sin\theta 3 & \cos\theta 3 & 0 & 0 \\ 0 & 0 & 1 & 0 \\ 0 & 0 & 0 & 1 \end{bmatrix}
$$

$$
{}^{3}_{4}T = \begin{bmatrix} \cos\theta 4 & -\sin\theta 4 & 0 & L3 \\ \sin\theta 4 & \cos\theta 4 & 0 & 0 \\ 0 & 0 & 1 & 0 \\ 0 & 0 & 0 & 1 \end{bmatrix}
$$

By inverse kinematics unknown angles can be calculated. $^{0}_{4}T$ matrix will be its overall transformation matrix; its fourth column is of linear transformation, as the designed mechanism is closed form so its end points are fixed. By using inverse kinematic technique unknown angles can be calculated. Fourth column elements are equal to the fixed points as the designed mechanism is closed chain. From final transformation matrix we get two equations (3.11) and (3.12).

L3cosθ1cosθ2cosθ3+L2cosθ1cosθ2-L3cosθ3sinθ2sinθ1-L2sinθ1sinθ2-
L3cosθ1sinθ3sinθ2 -L3sinθ1cosθ2sinθ3+L1cosθ1= Px   (3.11)

L3cosθ1sinθ2cosθ3 + L2cosθ1sinθ2+ L3sinθ1cosθ2cosθ3 + L2sinθ1cosθ2 +
L3cosθ1cosθ2sinθ3 -L3sinθ1sinθ2sinθ3+L1sinθ1= Py   (3.12)

L1, L2, L3 are link lengths, θ_1, θ_2, θ_3 are link angles and Px, Py are fixed points of link 3. Solving these equation unknown angles can be calculated.

Above designed mechanism has following link lengths and fixed points L1=12.5mm, L2=58mm, L3=36mm, P_x=75mm, P_y=0.12. For each degree change in θ1 there is a unique value of θ2 and θ3.
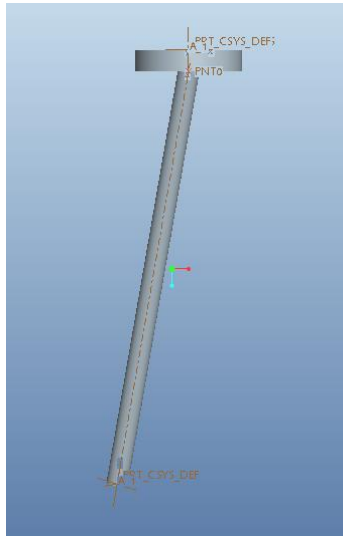
3.5 Three Link 3 D Mechanism

Figure 3-7 Designed three link mechanism

A link with single spherical joint is designed using DH approach to find spherical angles as shown in the figure 3-7. DH table for spherical joint is given in table 3-3. One end of the link is moved in a circle of known diameter so the end points are fixed and known, other end is connected to ground with spherical joint as shown in the figure 3-8. Unknown angles can be calculated by inverse kinematic approach.
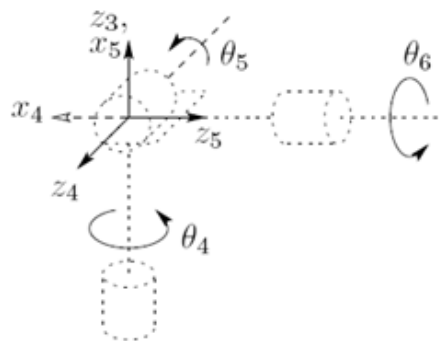
Figure 3-8 Spherical joint

3.5.1 DH Table

DH table for 3 link 3 D mechanism is given in table 3-3.

Table 3-3 DH table for three link 3D mechanism

i	α_{i-1}	a_{i-1}	d_i	θ_i
1	-90	0	0	θ_1
2	90	0	0	θ_2
3	0	0	0	θ_3
4	0	L	0	θ_4

3.5.2 Transformation Matrices

Transformation matrices for above designed mechanism are;

$$
{}^0_1T = \begin{bmatrix} \cos\theta 1 & -\sin\theta 1 & 0 & 0 \\ 0 & 0 & 1 & 0 \\ -\sin\theta 1 & \cos\theta 1 & 0 & 0 \\ 0 & 0 & 0 & 1 \end{bmatrix}
$$

$$
{}^1_2T = \begin{bmatrix} \cos\theta 2 & -\sin\theta 2 & 0 & 0 \\ 0 & 0 & -1 & 0 \\ \sin\theta 2 & \cos\theta 2 & 0 & 0 \\ 0 & 0 & 0 & 1 \end{bmatrix}
$$

$$
{}^2_3T = \begin{bmatrix} \cos\theta 3 & -\sin\theta 3 & 0 & 0 \\ \sin\theta 3 & \cos\theta 3 & 0 & 0 \\ 0 & 0 & 1 & 0 \\ 0 & 0 & 0 & 1 \end{bmatrix}
$$

$$
{}^3_4T = \begin{bmatrix} \cos\theta 4 & -\sin\theta 4 & 0 & L \\ \sin\theta 4 & \cos\theta 4 & 0 & 0 \\ 0 & 0 & 1 & 0 \\ 0 & 0 & 0 & 1 \end{bmatrix}
$$

Equating the overall transformation matrix column four with known points, unknown spherical angles can be calculated.

$$L\cos\theta1\cos\theta2\cos\theta3 - L\cos\theta1\sin\theta2\sin\theta3 \quad = \quad Px \quad\quad\quad (3.13)$$

$$L\sin\theta2\cos\theta3 + L\cos\theta2\sin\theta3 = \quad Py \quad\quad\quad (3.14)$$

$$-L\sin\theta1\cos\theta2\cos\theta3 + L\sin\theta1\sin\theta2\sin\theta3 \quad = \quad Pz \quad\quad\quad (3.15)$$

L is link length, $\theta1$, $\theta2$, $\theta3$ are spherical angles and Px, Py and Pz are fixed points. Solving these equation unknown angles can be calculated. Above designed mechanism has a link length of L = 42mm, and radius of disk r= 12.5mm, and fixed points Px = rcosθ, Py = rsinθ, and Pz=48.42. For each degree change in input θ there is a unique value of $\theta1$, $\theta2$, $\theta3$.

Results of mathematical modeling and commercial codes are compared to verify the mathematical results. Figure 3-9 and figure 3-10 are position plots, we can see peak to peak values are same but not the absolute values because software and mathematical modeling coordinate placement positions are different, however results are same because amplitude is same. DH result of position plot is shown in figure 3-11, points are taken from the transformation matrix $_8^0 T$ and plotted. Comparing peak to peak values is giving error percentage of 1.1%. This is because in DH approach we are modeling spherical joint as a combination of three revolute joints. Two spherical joints are modeled in series resulting in another degree of freedom that is the rod start spinning around its axis. This extra degree of freedom produces variations in results, so points have been chosen and plotted in the figure 3-11.
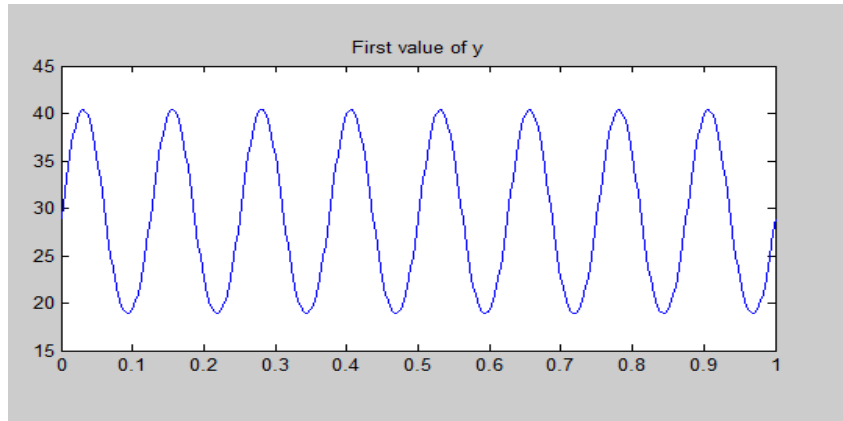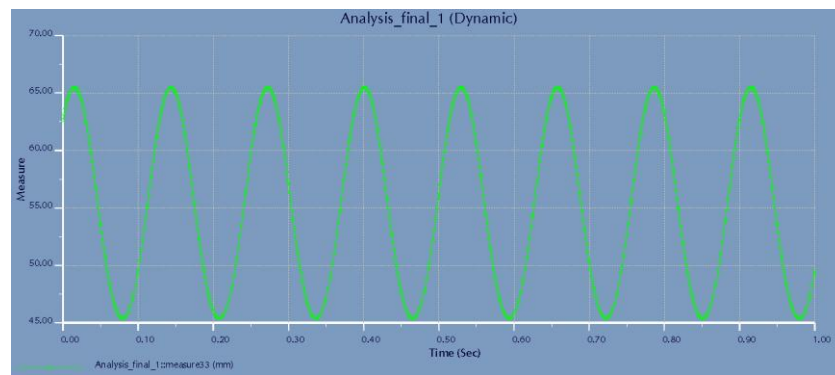
Figure 3-9 Position plot by computed values
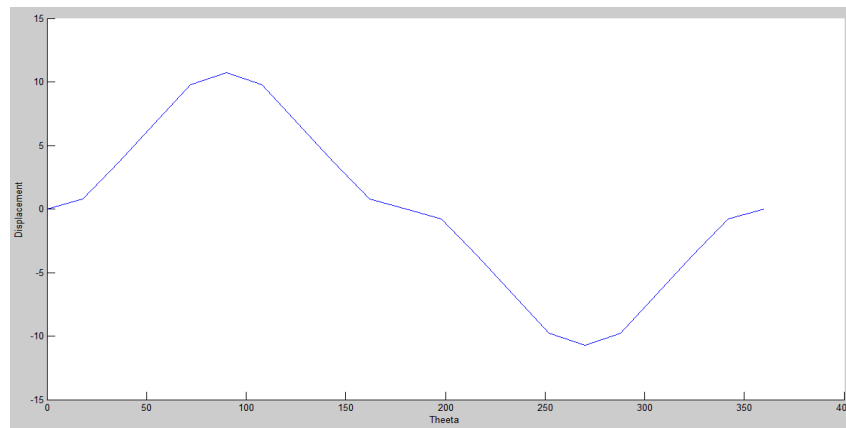

Figure 3-10 Position plot by software

Figure 3-11 Position plot of DH values

Above position plots, loop closure equations and software plots, are on 8 Hz and that of DH approach is based on changing theta of crank. Figure 3-12, figure 3-13 and figure 3-14 shows position plots of software, loop closure approach and DH approach respectively of single cycle in time domain.
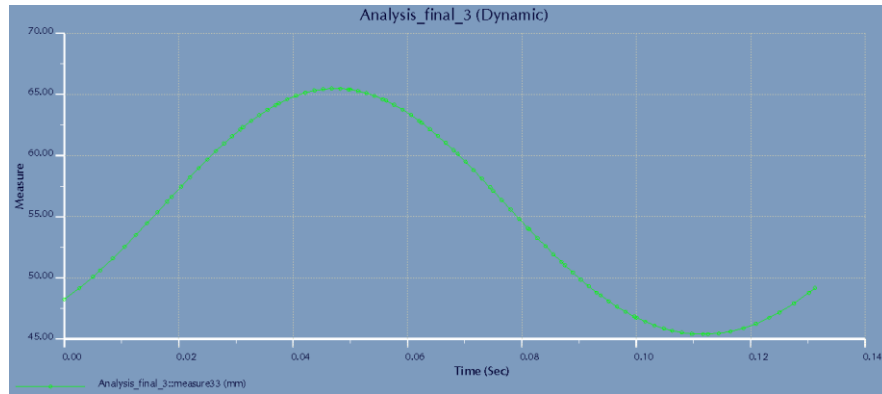
34

Figure 3-12 Position plot of flapping link (software result)
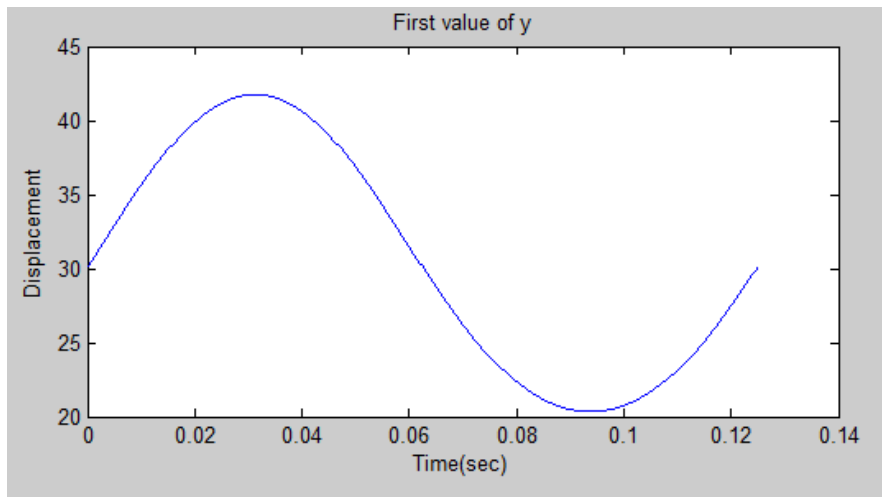
Figure 3-13 Position plot of flapping link (Loop closure equation result)
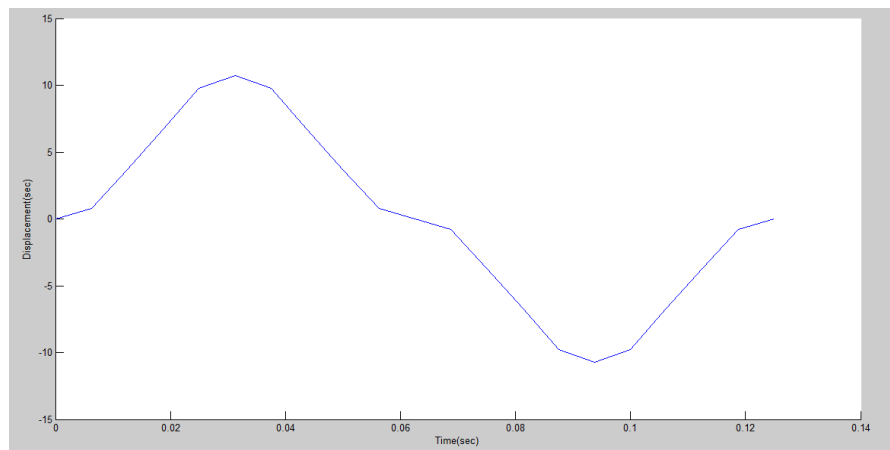
Figure 3-14 Position plot of flapping link (DH result)

35

Computed and software results of velocity plot are shown in figure 3-15. Velocity is maximum at the mean position and minimum at extreme position. The amplitude difference between two waveforms is 4.5mm/sec with error percentage of 1.2% which can be due to a minor difference of link length between software and mathematical results, in software three dimensional models are being analyzed while in mathematical calculations points and vectors are being used.
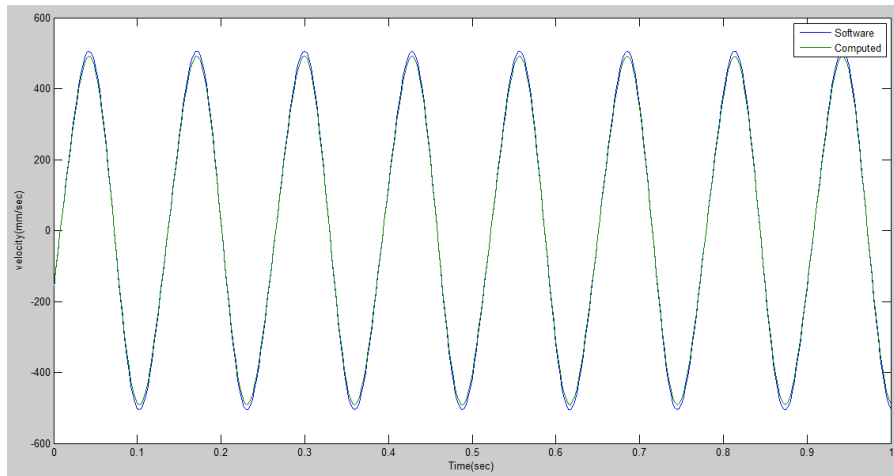
Figure 3-15 Velocity plot of flapping link

Chapter 4: Prototype

Chapter 4: Prototype

A scaled up prototype is fabricated to verify the functionality of designed mechanism. Fabricated prototype is an experimental setup for measuring power requirements of flap. Prototype is first designed in software then fabricated. Designed prototype is shown in the figure 4-1.
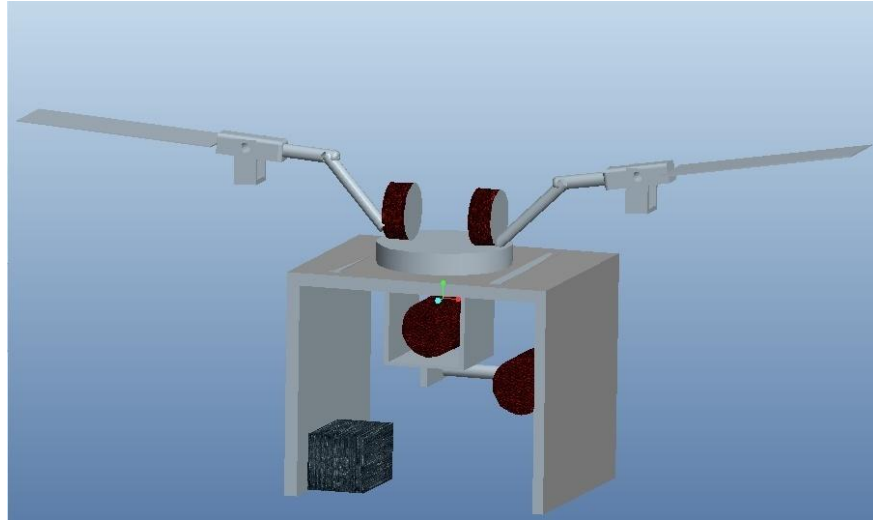
Figure 4-1 Prototype designed in Pro E

Prototype is fabricated in local workshop, consisting of two DC motors, battery, and links made up of aluminum and steel. Fabricated prototype is shown in the figure 4-2.
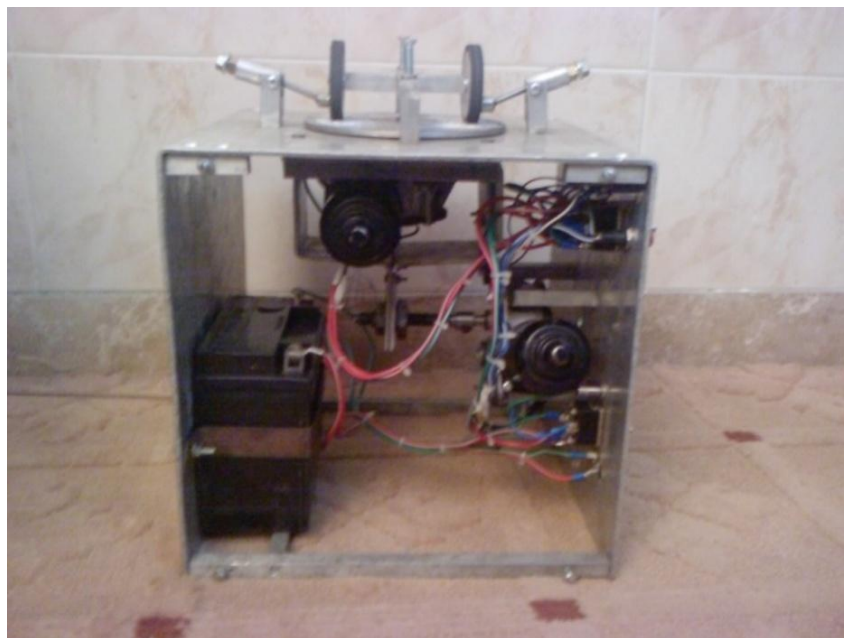
Figure 4-2 Prototype fabricated

Rotating disk is driving the mechanism and is made up of steel. Rotating wheels are of aluminum with rubber molded on then. Disk and wheels are frictionally in contact with each other. According to the concept disk should move from its mean position to some distance to vary the speed of rotating wheels which will ultimately change the frequency of flap, to achieve this two motors have been installed motor M1 to give drive to the disk and motor M2 to move the disk left or right from mean position. Both motor are of 12 V 30 Watts. Figure 4-3 shows the fabricated mechanism.
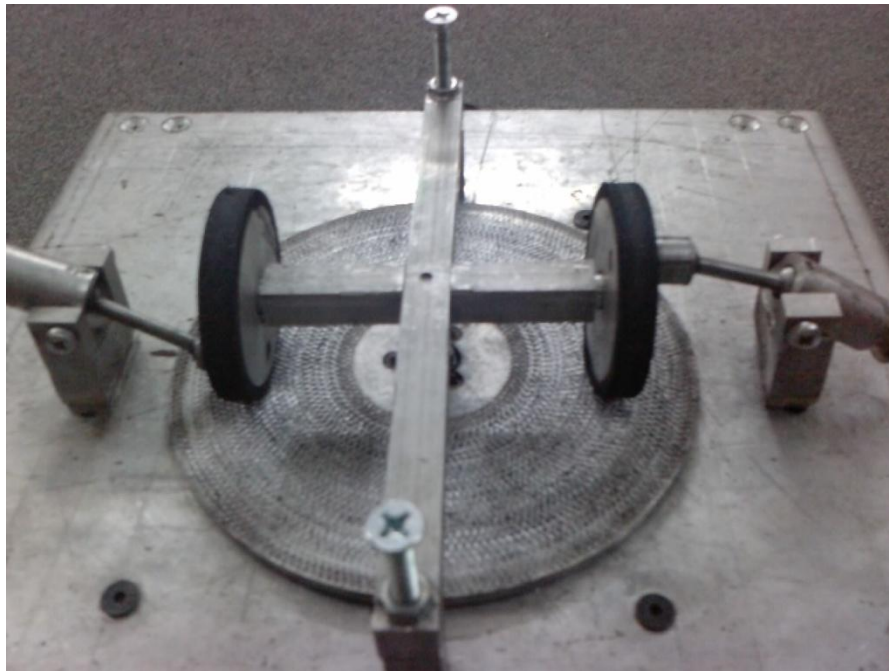
Figure 4-3 Designed mechanism

These motors are being controlled by simple switches and a push button. Battery used is of 12 V, 8 Ampere rechargeable. All driving mechanism is installed in an aluminum box.

4.1 Parametric Study

Parametric study of fabricated mechanism is carried out to determine the effects of link lengths on the position of L_4. A change in position of L_4 is studied by changing the link lengths one by one. Schematic diagram of the designed mechanism is shown below in figure 4-4.

Figure 4-4 Schematic diagram of mechanism

Link lengths of fabricated mechanism are

L_1 = 42mm, L_2=30mm, L_3 = 45mm, L_4 = 3mm.

These link lengths are chosen keeping in view Grashof condition and desired motion. Position plot for the mechanism is shown in the figure 4-5.
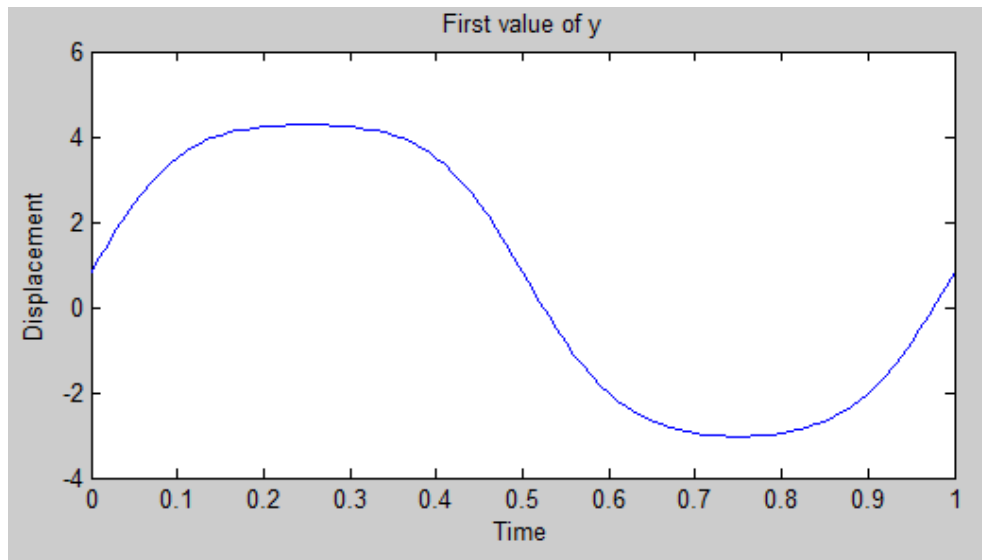

Figure 4-5 Position plot of mechanism

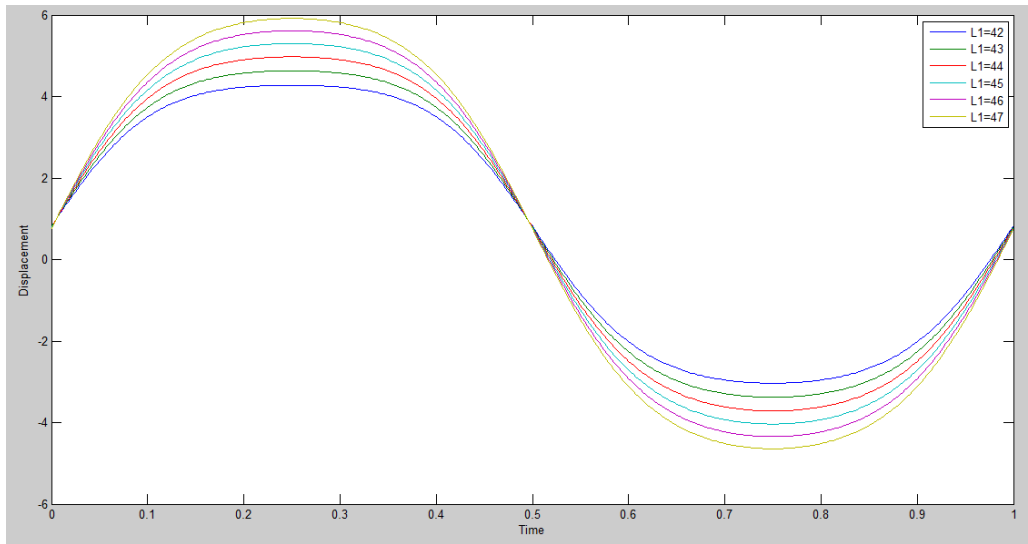We will start with L_1. If the L_1 is increases flap increases and if decreased flap decreases as shown in figure 4-6.

Figure 4-6 Parametric study of L1

If link L_2 is decreased output flap decreases and if increased flap increases as shown in figure 4-7.
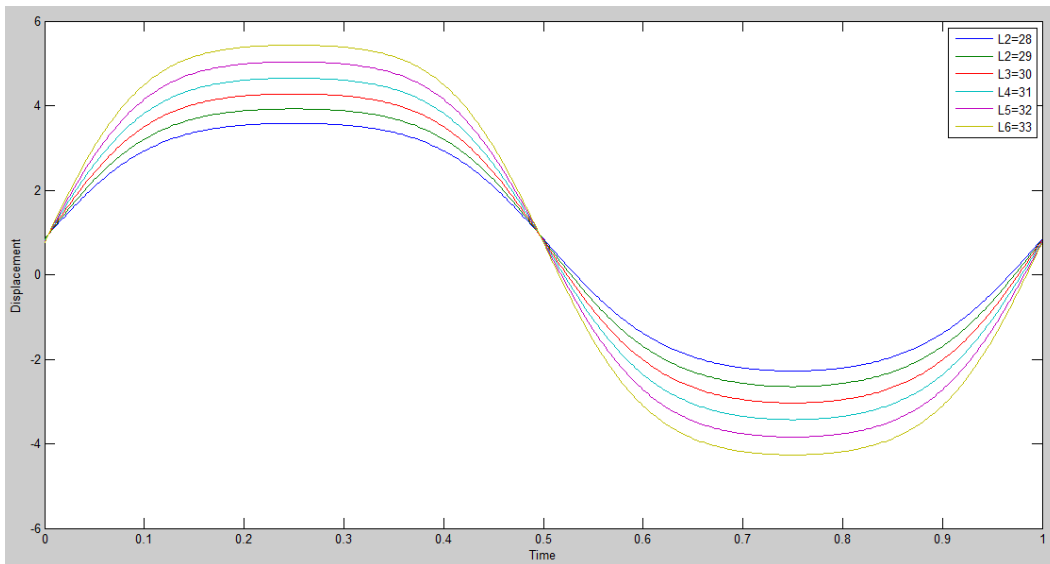

Figure 4-7 Parametric study of L2

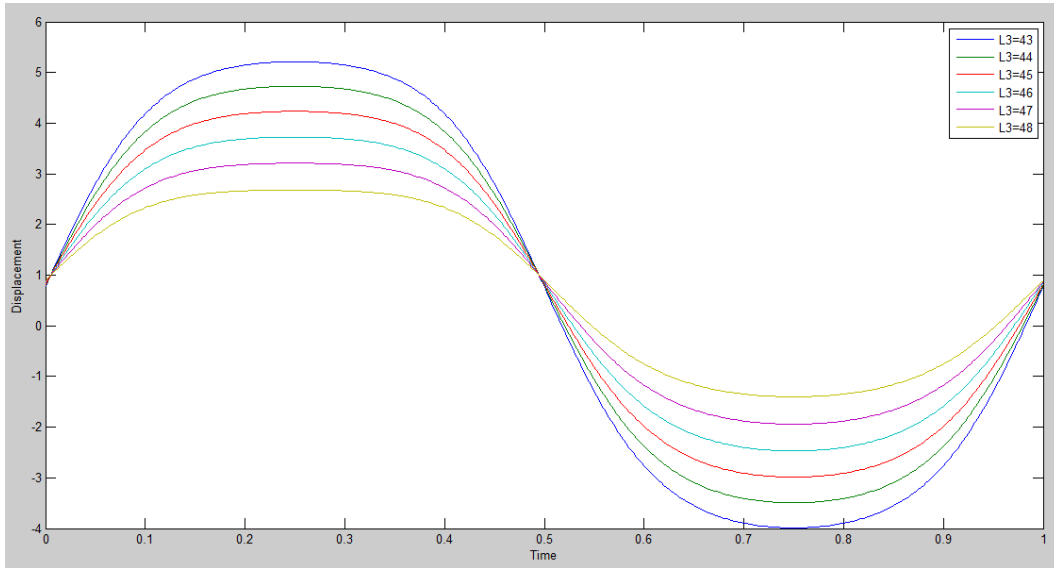If L_3 is increased flap amplitude decreases and if it is decreased flap amplitude increases as shown in figure 4-8.

Figure 4-8 Parametric study of L3

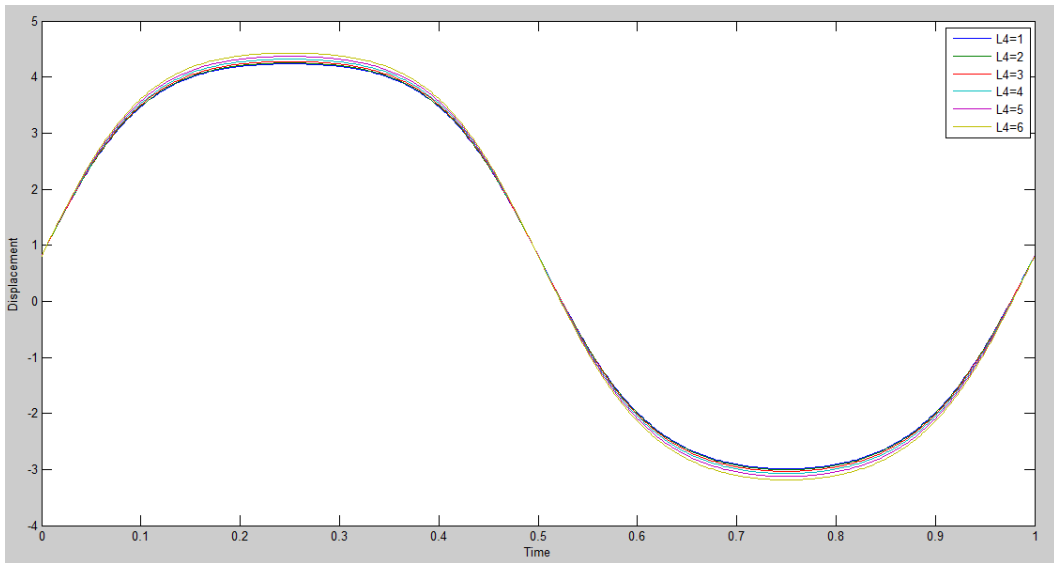If L_4 is increased flap amplitude decreases and if decreased flap amplitude increases as shown in figure 4-9.

Figure 4-9 Parametric study of L4

4.2 Experiment

An experiment is performed on prototype. Power of M1 motor is observed for different offsets of disk from center, as the distance of wheel changes from center of rotation frequencies of wings varies as shown in figure 4-10.
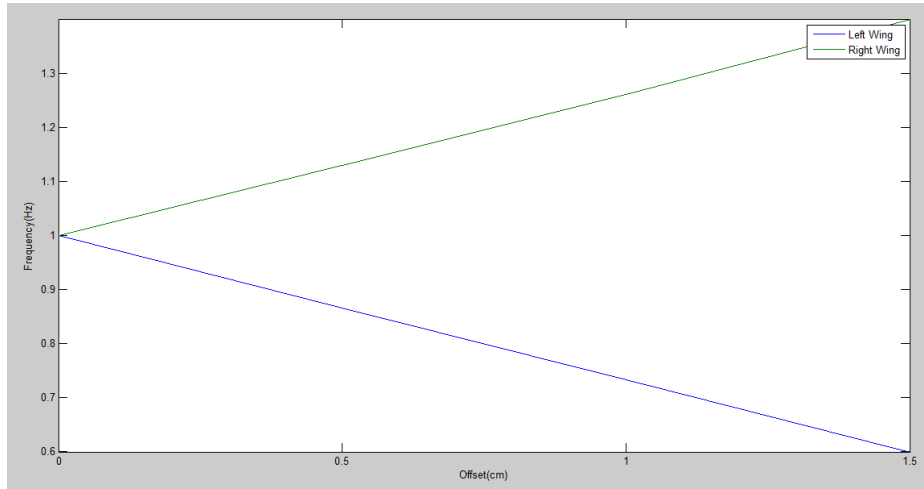

Figure 4-10 Frequencies of wings with disk offset

As distance of disk from the center increases current decreases, because asymmetrical flap helps to maintain the uniform motor torque, and hence reduces load on motor [13]. If we disassemble one side and experiment with only one wing then power is directly proportional to wheel rpm. Disk can move a maximum offset of 1.5 cm from the center. Results are shown in table 4-1. Positive and negative direction offset is shown in figure 4-11.
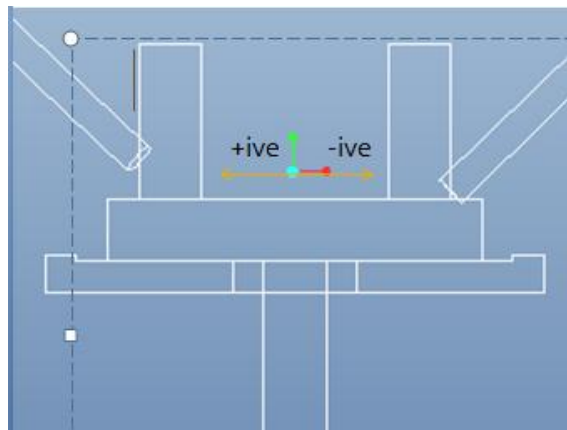

Figure 4-11 Offset direction

43

Table 4-1 Power calculation of M1

S#	Offset (cm)	Power to Rotate disk (Watt)	Power to rotate Wheels (Watt)	Power to run Mechanism (Watt)	Power to Flap (Watt)	Power to Flap (Pro-E) (Watt)
1	0	10.45	2.38	13.3	.48	.34
2	0.5	8.16	2.0	10.54	.38	.28
3	1	8.03	1.72	10.07	.32	.23
4	1.5	7.51	1.4	9.21	.28	.19

Power to flap measured is more than the software because in measured power there is joint friction as well. Variation of power with offset of disk is shown in figure 4-12. Power reduces as the offset increases because asymmetrical flap helps to maintain the uniform motor torque, thereby reducing load on the motor and hence power requirements [13].
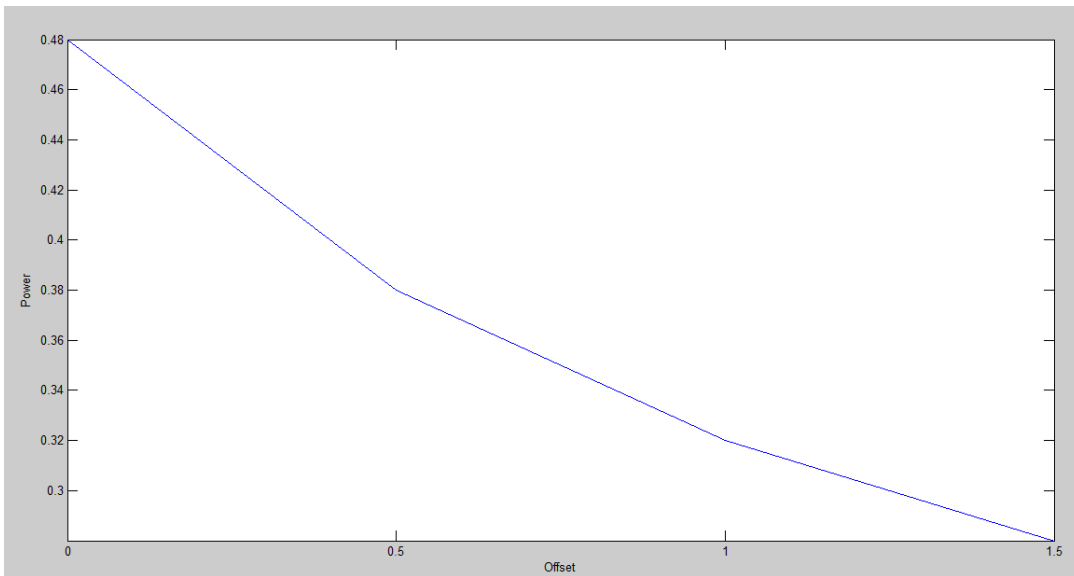

Figure 4-12 Offset vs power plot

Mechanism is experimented for power calculation, in these calculations we come across different type of power losses mainly wiring losses, core losses, winding losses, stray losses and mechanical losses.

Overall resistance in electrical connections is measured and wiring loss calculated which comes put to be 8.78Watt. Core and winding losses for motor is 3Watt. Mechanical and stray losses are about 1 Watt.

The prototype can successfully vary the frequencies of wings; we can use this setup to measure the power requirements of flap. Different wing can be tested on this test bench for power requirements of flap.

Chapter 5: Results

Chapter 5: Results

5.1 Kinematic Analysis

Kinematic analysis is performed to study the mechanism position, velocity and acceleration without considering the forces causing movements. Kinematic analysis of designed mechanism is performed in Pro Engineer; results are discussed in this chapter. Pro E model of mechanism is shown in figure 5-1.
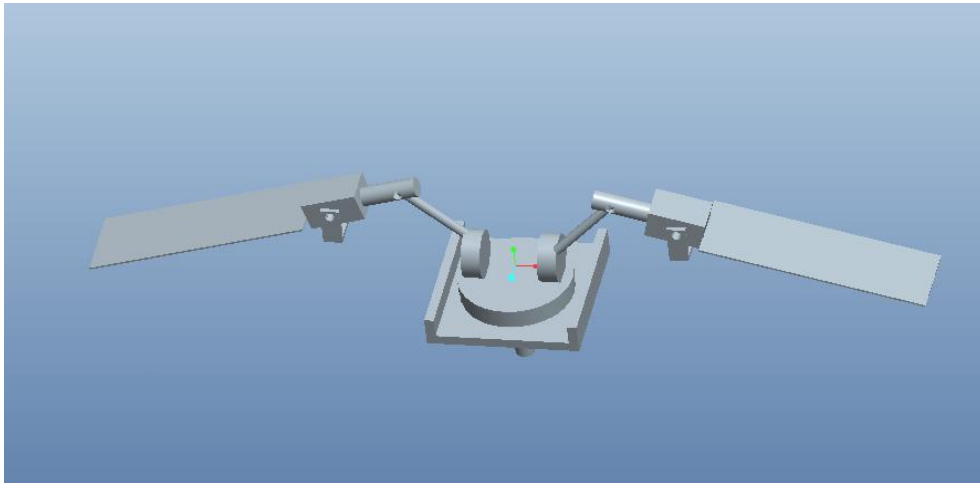

Figure 5-1 Pro E model of mechanism

Mechanism in simulated at frequency of 8 Hz. The plot in figure 5-2 is the position of wing in time span of 1 sec. The wing flaps 8 times in one second, and is a sinusoidal curve. Considering one complete cycle wing first starts flapping up reaches its maximum position, flap down and complete its first cycle.
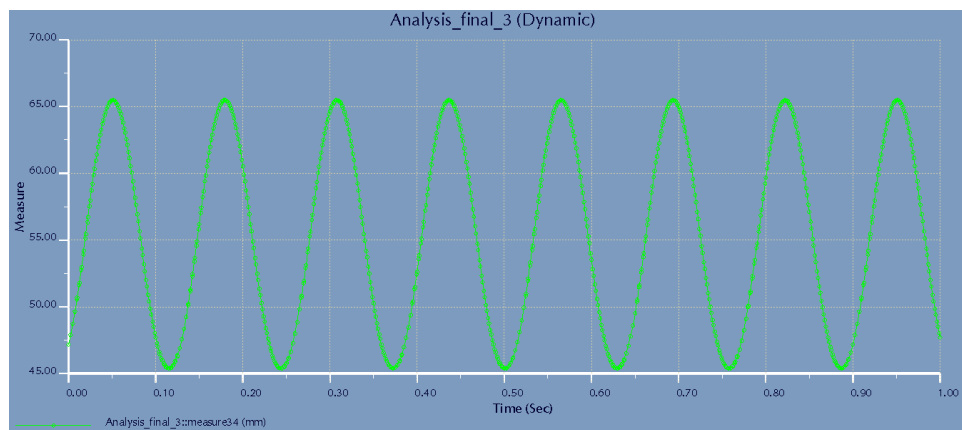

Figure 5-2 Position plot of wing

Velocity plot of wing is shown in figure 5-3. As wing starts flapping its velocity starts increasing, is maximum at mean position, starts decreasing and zero at extreme position.
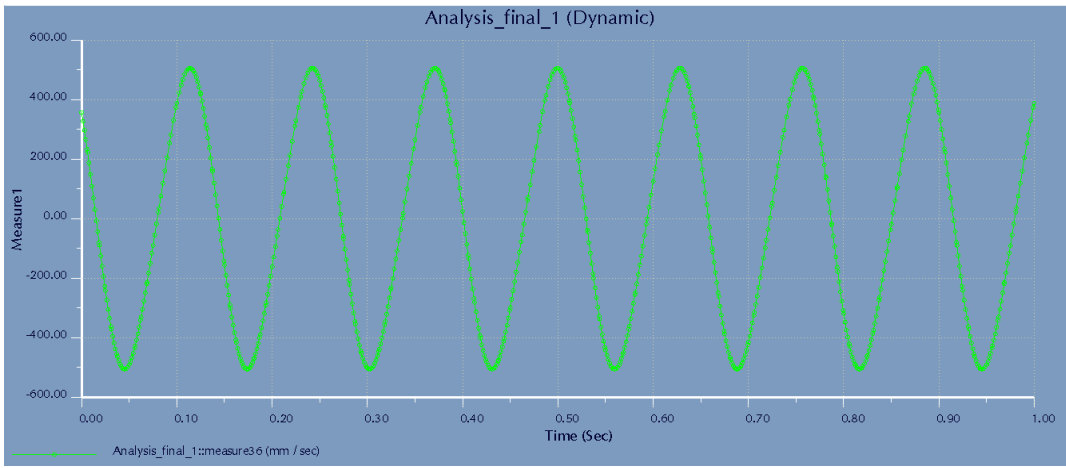

Figure 5-3 Velocity plot of wing

Acceleration plot is shown in figure 5-4. As wing starts' flapping up its rate of change in velocity is maximum. Acceleration is maximum at extreme positions and minimum at mean position. At 8 Hz frequency maximum acceleration is 20000 mm/sec^2 and is sinusoidal. Time delay in positive peak is more than negative peak because flap link is at 24mm offset from crank axis.
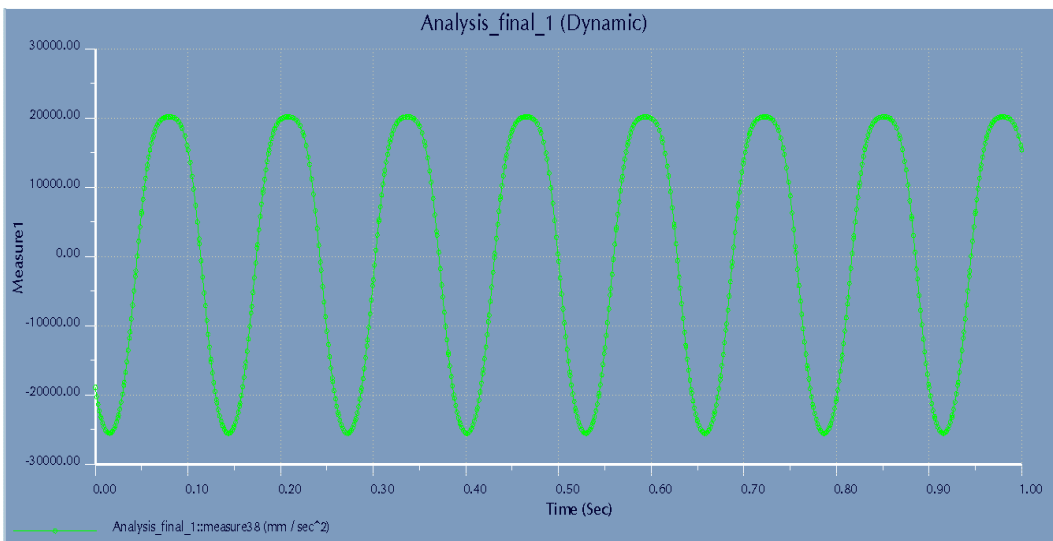

Figure 5-4 Acceleration plot of wing

Angular position plot of wing is shown in figure 5-5. For the particular position of linkages wing flaps 22 degree up and 10 degree down. These angular positions can be changed by varying link lengths, distances and offsets.
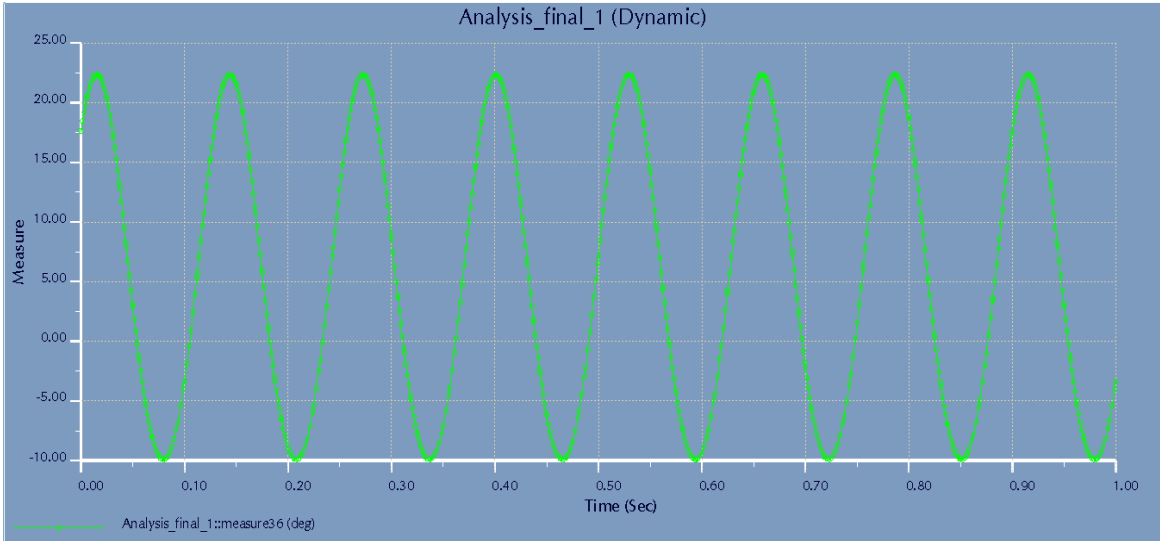

Figure 5-5 Angular position plot of wing

Angular velocity plot of wing is shown in figure 5-6. As wing starts flapping its angular velocity starts increasing, is maximum at mean position, starts decreasing and zero at extreme position. It is sinusoidal having maximum value of 800deg/sec.
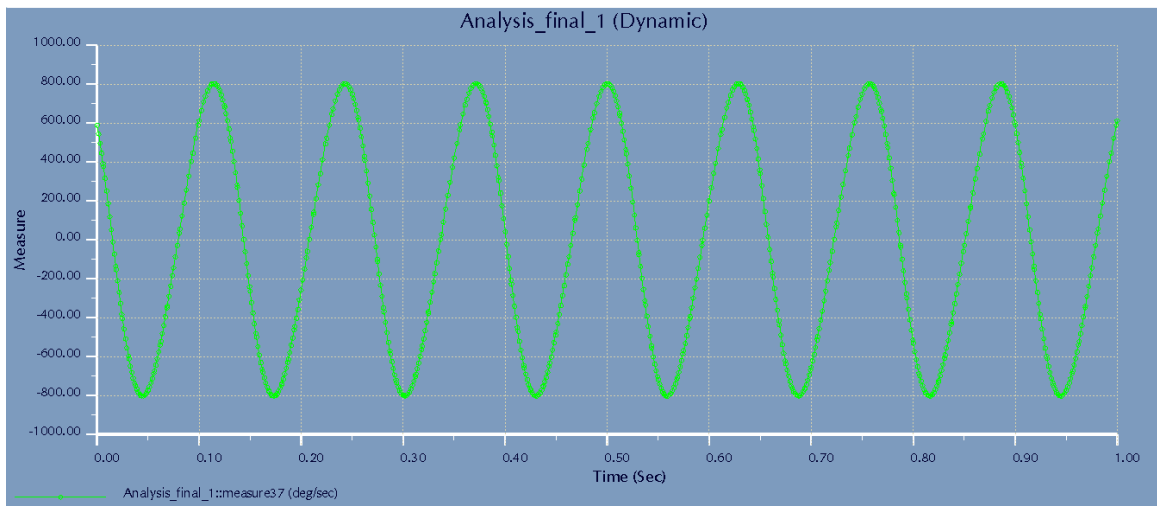

Figure 5-6 Angular velocity plot of wing

Angular acceleration plot of wing is shown in figure 5-7. As wing starts' flapping up its rate of change in angular velocity is maximum. Angular acceleration is maximum at

extreme positions and minimum at mean position. Time delay in positive peak is more than negative peak because flap link is at 24mm offset from crank axis. Angular acceleration is sinusoidal having maximum value of 32224deg/sec [2].
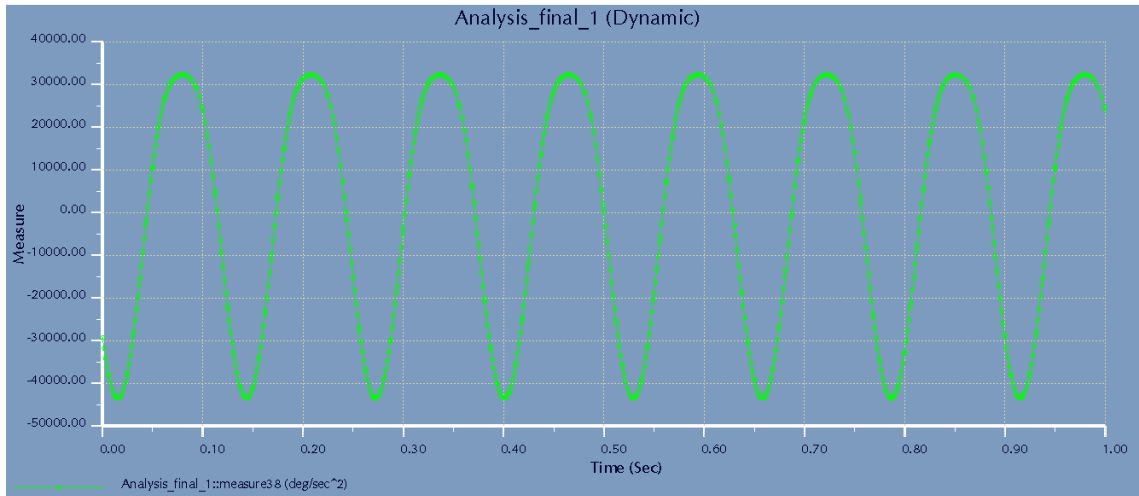

Figure 5-7 Angular acceleration plot of wing

Kinematic analysis is necessary for a good mechanism design. Studying position, velocities and acceleration helps in achieving desired position and motion. As the distance of crank disks changes form the center of friction disk angular velocity changes accordingly, resulting in a differential shift in the flapping frequency of wings. Let us consider the case in which one side frequency increases from 8 Hz and on other side decreases from 8Hz, with increasing frequency velocity and acceleration magnitude increases but position amplitude remain the same. Position amplitude changes with changing link lengths, the only change in position with increasing or decreasing frequency is the time to complete one complete cycle.

5.2 Parametric Study of Mechanism

Parametric study of mechanism is carried out to determine the effects of link lengths on the position of flap link. A change in position of L_4 is studied by changing the link lengths one by one. Schematic diagram of the designed mechanism is shown below in figure 5-8.
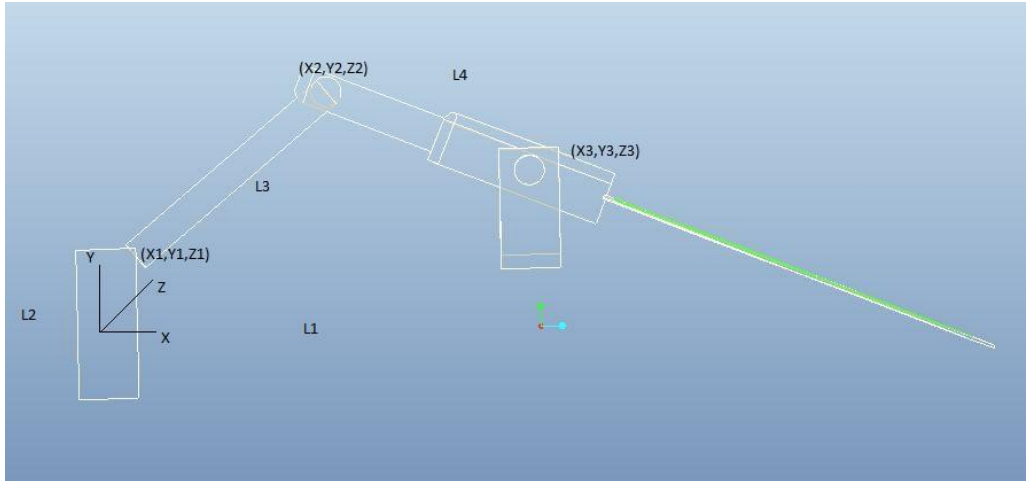
Figure 5-8 Schematic diagram of mechanism

Link lengths of the mechanism are

L_1 = 71mm, L_2=12.5mm, L_3 = 42mm, L_4 = 36mm.

These link lengths are chosen keeping in view Grashof condition and desired motion. We will start with L_1. L_1 is combination of horizontal and vertical movement which is studied separately. If the L_1 is increased in horizontal direction the flap increases and if decreased flap decreases as shown in figure 5-9. Not only the magnitude is increasing, flap link is also shifting from its datum axis. Figure 5-10 shows amplitude of flap with increasing L_1, amplitude of flap link increases with increasing L_1 horizontally. Point shown in figure 4-9 shows maximum value of flap amplitude for link L_1= 76mm.
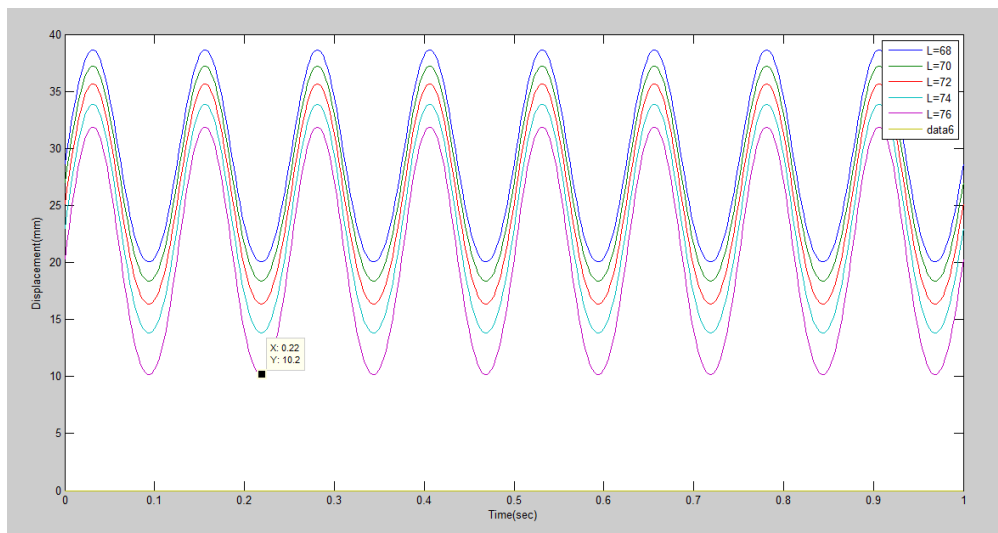

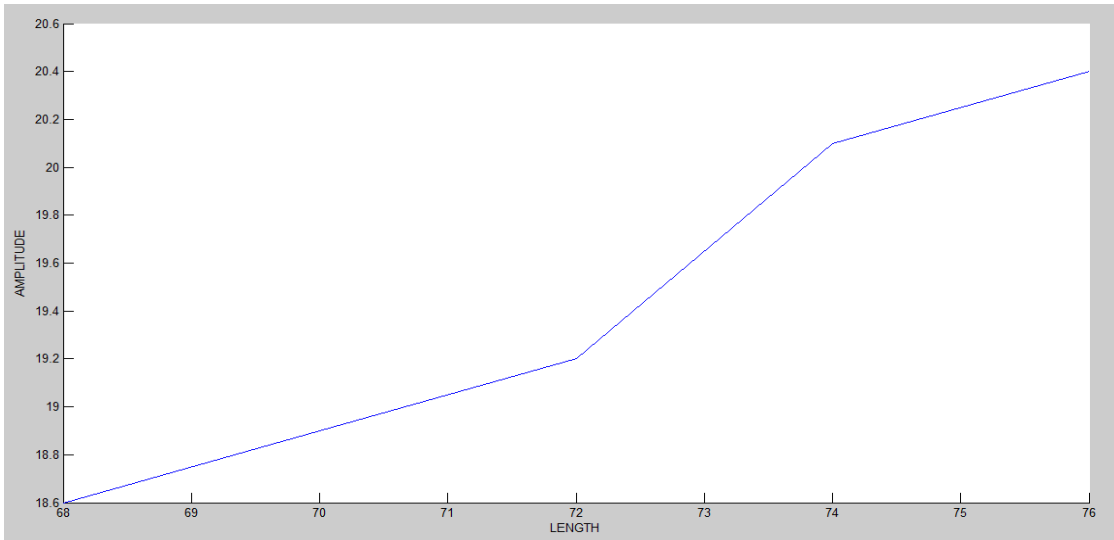**Figure 5-9 Parametric study of L1**

Figure 5-10 Amplitude vs L1

If the L_1 is increased in vertical direction the flap amplitude increases and if decreased flap amplitude decreases as shown in figure 5-11.
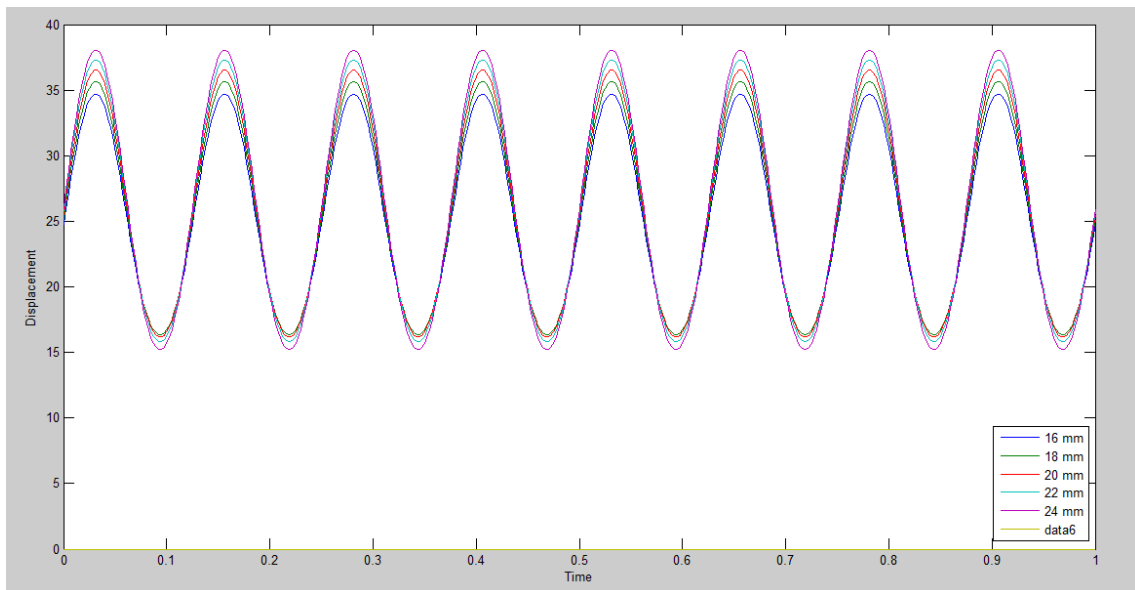

Figure 5-11 Parametric study of L1

Figure 5-12 shows amplitude of flap with increasing L_1, amplitude of flap link increases with increasing L_1 vertically.
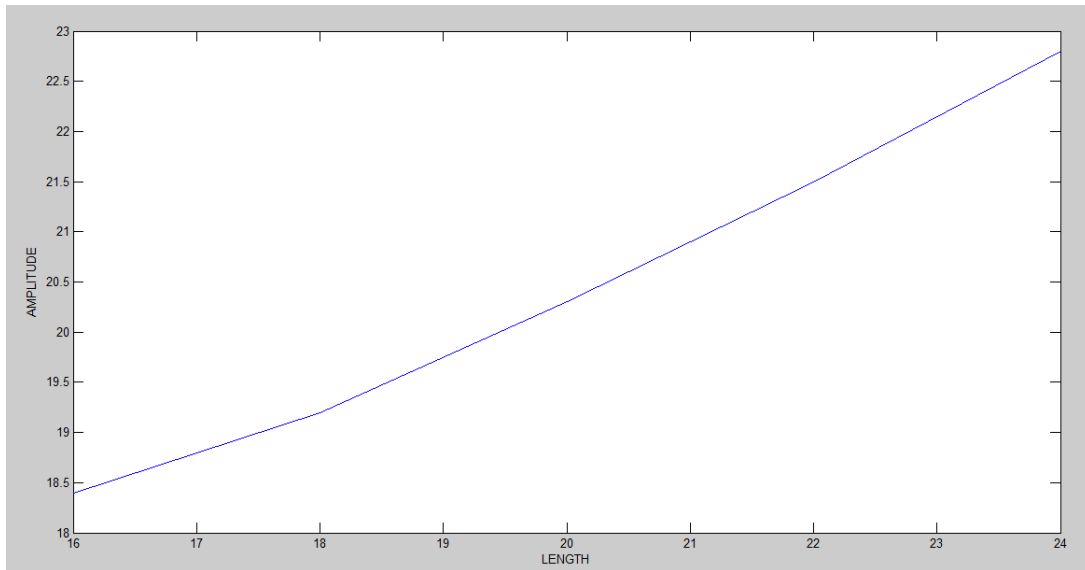

Figure 5-12 Amplitude vs L1

If link length 2 is decreased output flap decreases and if increased flap increases as shown in figure 5-13. Figure 5-14 shows the amplitude of flap with increasing L_2.
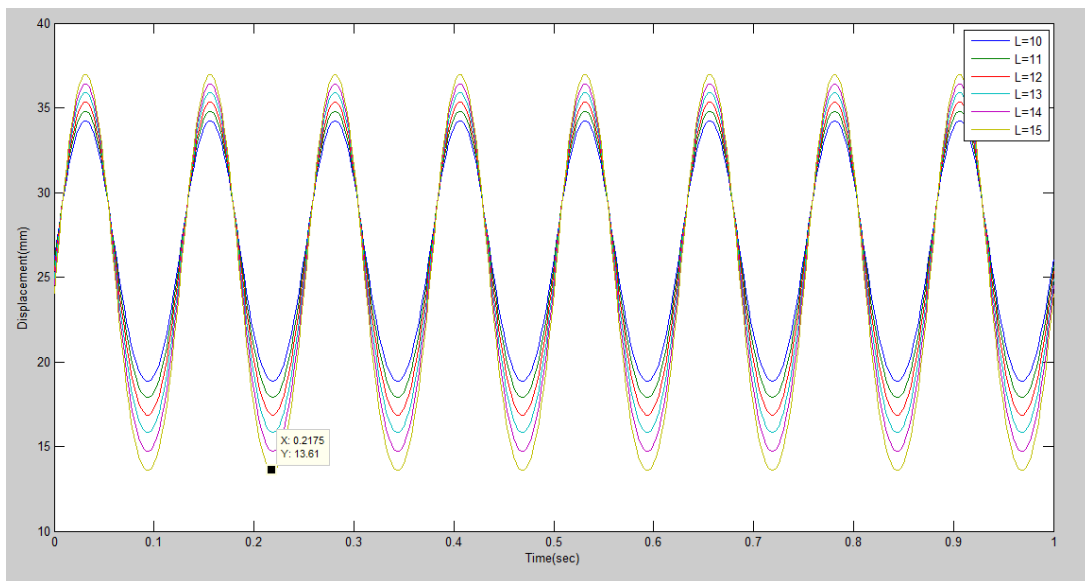

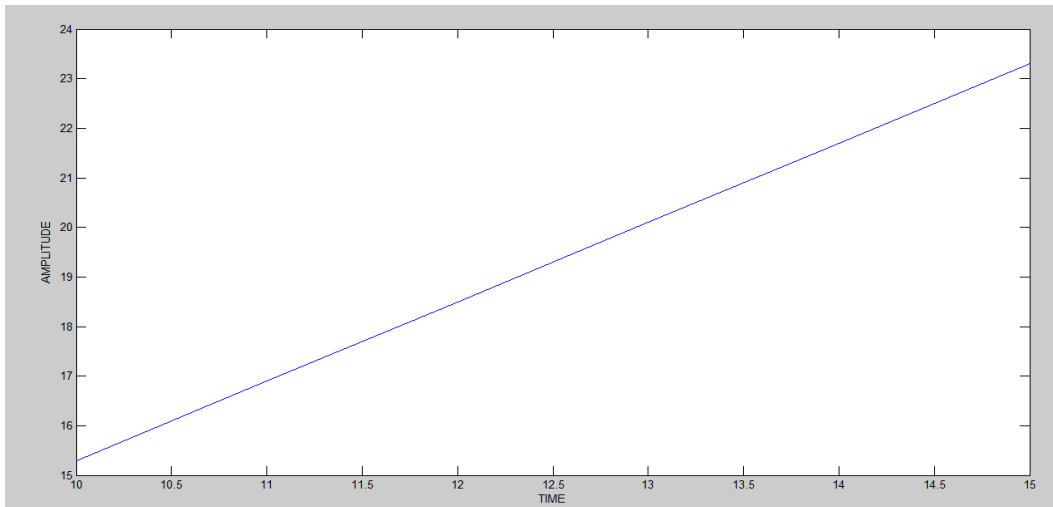**Figure 5-13 Parametric study of L2**

Figure 5-14 Amplitude vs L2

L_3 is connecting crank with rocker and is connected by spherical joints. If it is increased flap amplitude decreases and if it is decreased flap amplitude increases as shown in figure 5-15. Figure 5-16 shows the amplitude of flap with increasing L_3.

Figure 5-15 Parametric study of L3

Figure 5-16 Amplitude vs L3

If L_4 is increased flap amplitude decreases and if decreased flap amplitude increases as shown in figure 5-17. Figure 5-18 shows the amplitude of flap with increasing L_4.
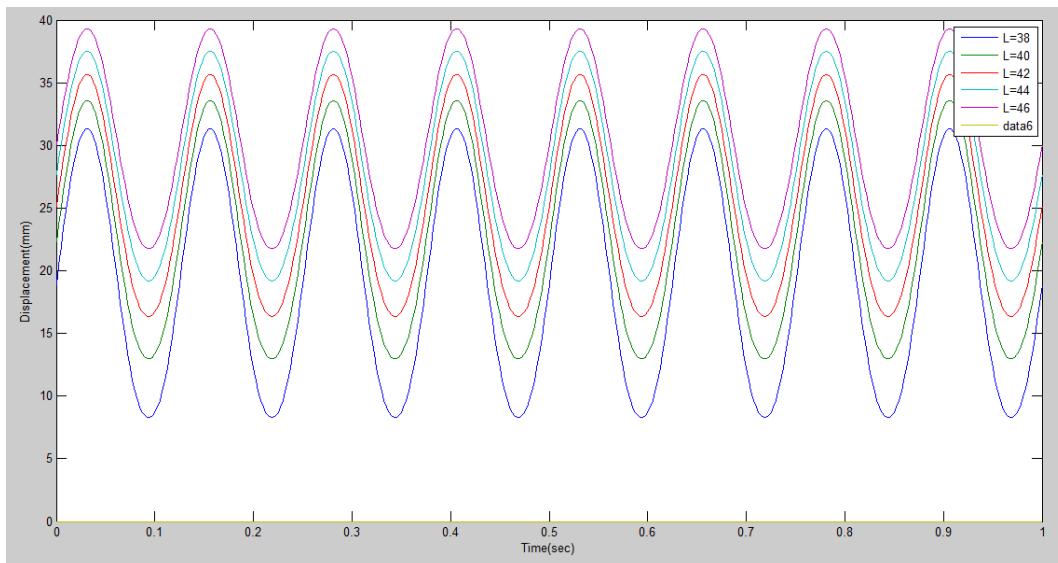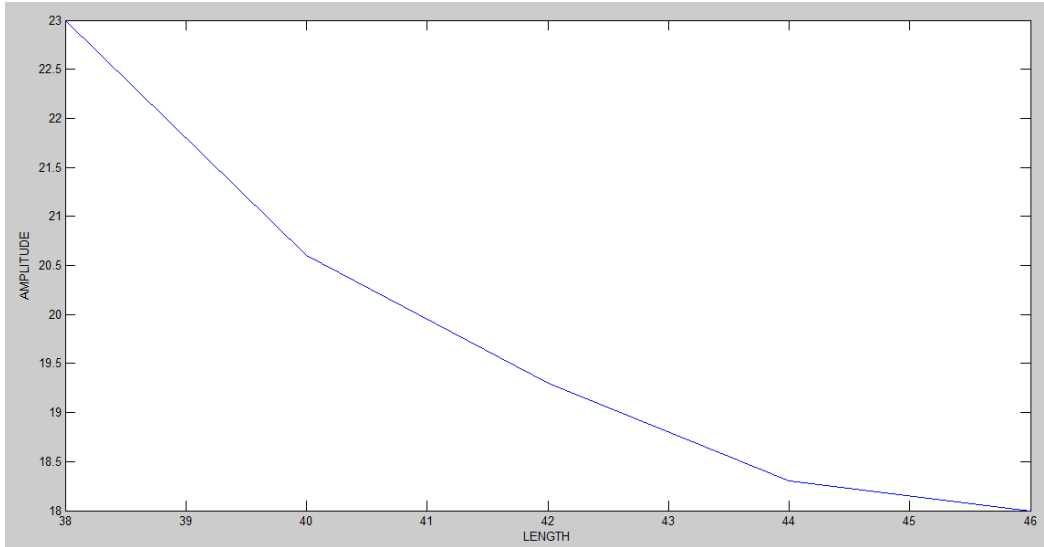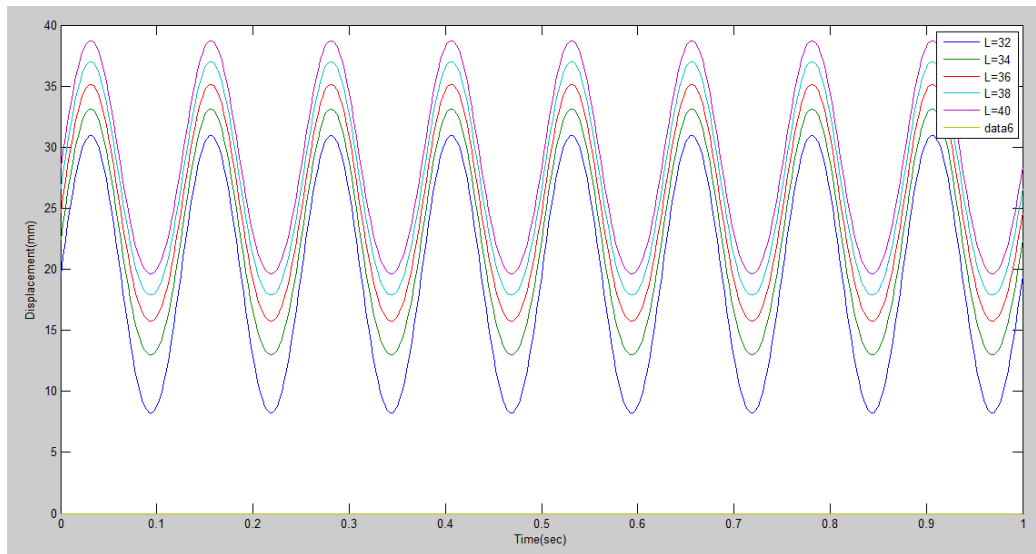

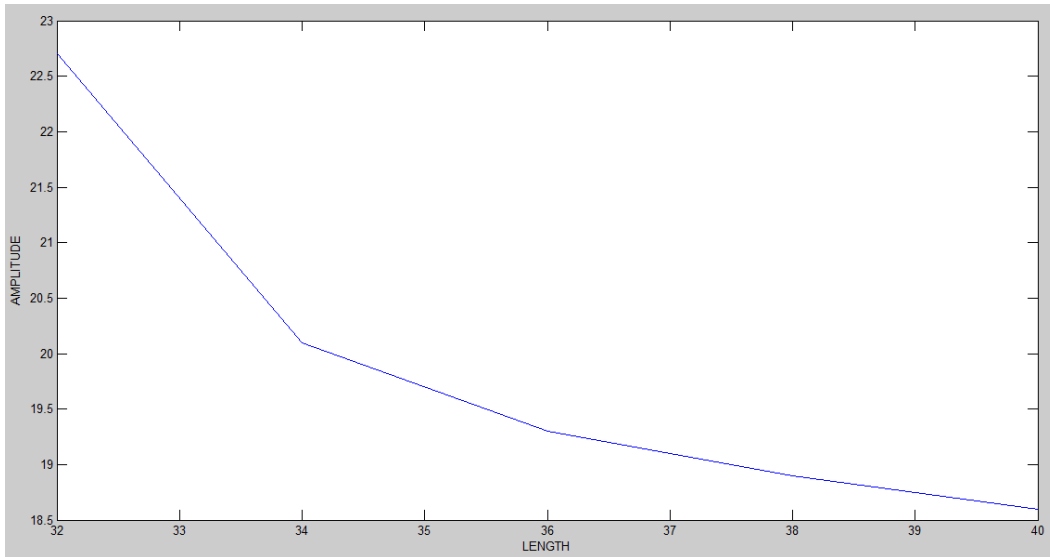**Figure 5-17 Parametric study of L4**

Figure 5-18 Amplitude vs L4

5.3 Dynamic Analysis

To find the power requirements of mechanism and forces on joints dynamic analysis is performed in Pro Engineer. By Dynamic analysis we can find power requirements of mechanism for a particular wing, power calculations from dynamic analysis will then be compared with experimentally measured power. Joint forces will help in improving design because we can design more efficient mechanism structure wise. These forces will help in selecting bearings, and designing supports. Dynamic results on wing joint and the joint connecting wing with connecting rod are discussed here. Mechanism is first modeled dynamically in software and then simulated. Analysis is performed with symmetric flapping frequency of 8 Hz.

5.3.1 Wing Joint

5.3.1.1 Radial Force (x axis)

A force exerted perpendicular to the object axis or centerline is radial force. As wing starts increasing its flapping angle positively radial force in x direction starts decreasing and is minimum near extreme position of wing and zero at extreme position as shown in the figure 5-19.
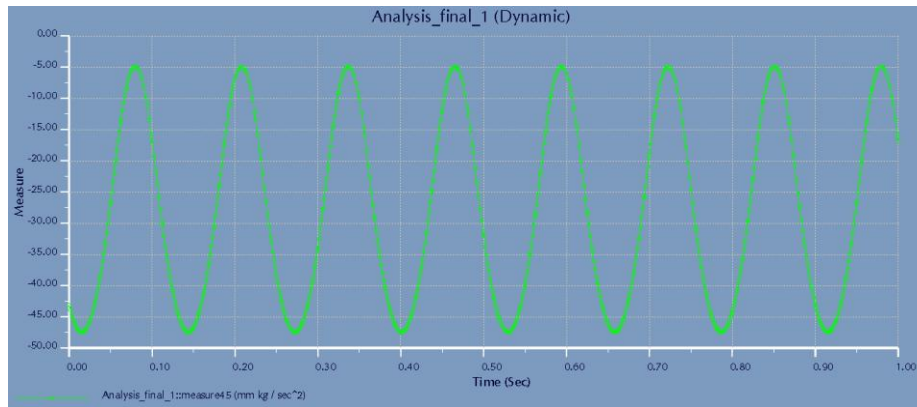
Figure 5-19 Radial force(x axis) on wing

5.3.1.2 Radial Force (y axis) on Wing Joint

As wing starts increasing its flapping angle (flapping up) radial force in y direction starts decreasing and is minimum at extreme position of wing as shown in the figure 5-20. It starts increasing again as wing flaps down and again decreases to minimum value for extreme position of wing in downward direction. Maximum values of radial force are 50mmkg/sec^2 and -25mmkg/sec^2, this asymetricity in magnitudes is due to the reason that flapping angle is asymmetric and wing has an offset with the crank position.
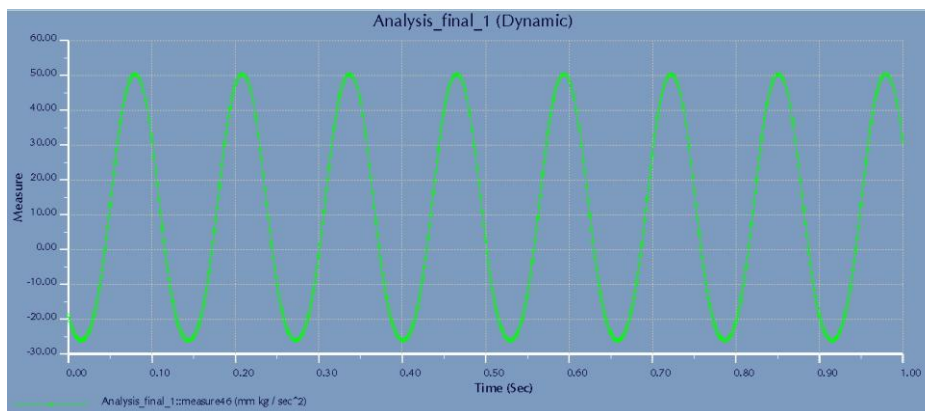

Figure 5-20 Radial force(y axis) on wing

5.3.1.3 Axial Force

A force that is applied through center of gravity of its cross section is called axial force, and the load is called axial load. If we consider a member axial force will be either compression or tension. If axial force is acting through centroid of body,

57

the loading will be concentric otherwise eccentric. Eccentric loading is responsible for producing moment in beams.

As wing starts increasing its flapping angle (flapping up) axial force starts increasing maximum at mean position and starts decreasing and is minimum at extreme position of wing as shown in the figure 5-21. For down flap it starts increasing again become maximum at mean position and starts decreasing up to extreme position having magnitude values of 7.683mmkg/sec^2. Axial force magnitude is increasing and decreasing two times in one cycle because flap link is being pulled by the connecting rod two times in z axis.

Figure 5-21 Axial force on wing

5.3.2 Connecting Rod (Spherical Joint)

5.3.2.1 Total Force in x Direction

Total force is combination of radial and axial component. For the total force in x direction it has maximum values at mean position and minimum at extreme positions. Total force in x direction magnitude is increasing and decreasing two times in one cycle because flap link is being pulled by the connecting rod two times in x axis as shown in figure 5-22.
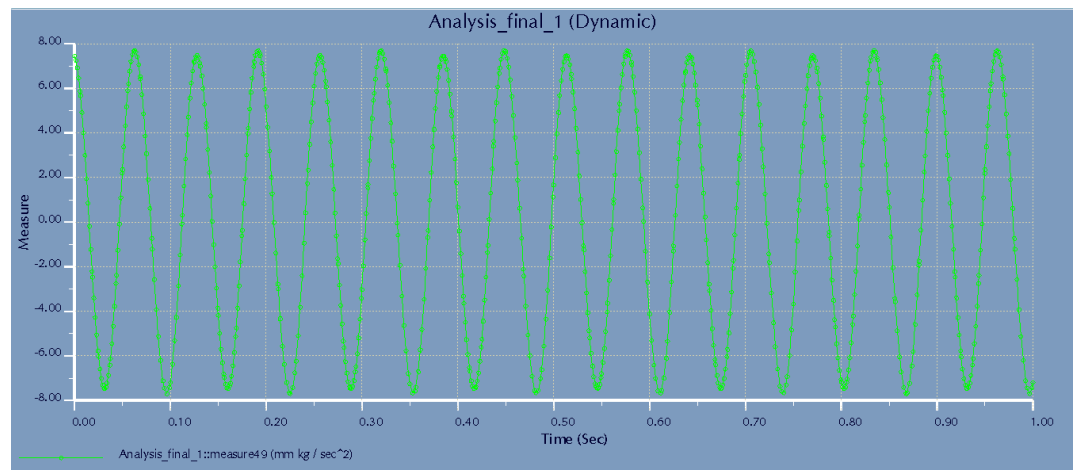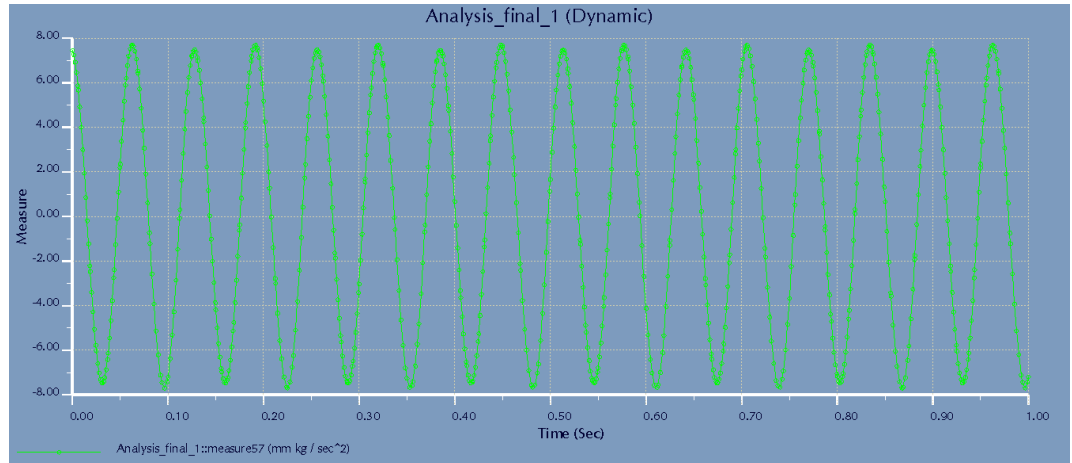
Figure 5-22 Total force in x direction

5.3.2.2 Total Force in y Direction
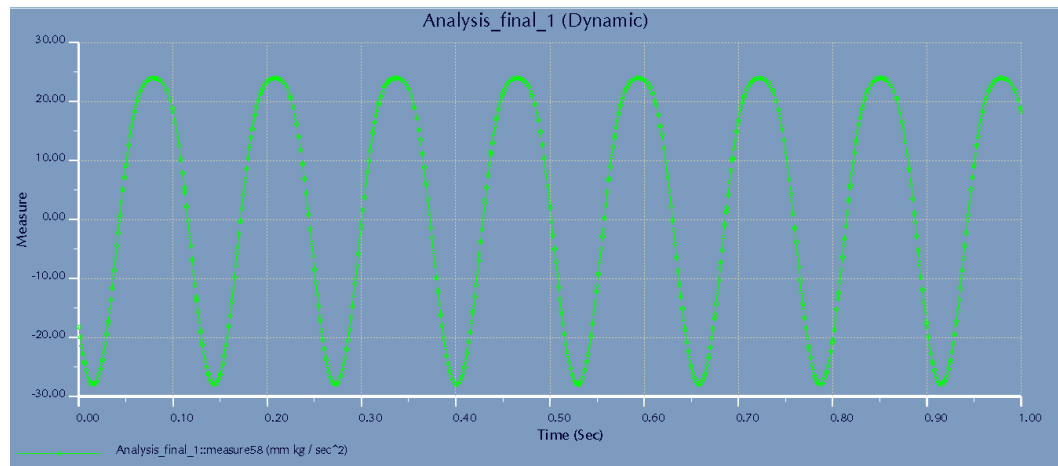
Figure 5-23   Total force in y direction

Total force in y direction is shown in figure 5-23. With the upward movement of wing total force decreases and is minimum at maximum upward flap, as it flaps down forces starts increasing reaches maximum value at near maximum downward flap and cycle continues. Time span for upward flap is more than downward as upward flap angle is more than downward because flap link joint axis is at offset from crank axis.

5.3.2.3 Total Force in z Axis

Total force in z direction is shown in figure 5-24. With the upward movement of wing total force decreases and is minimum at maximum upward flap, as it flaps

down forces starts increasing reaches maximum value at near maximum downward flap and cycle continues.

Figure 5-24 Total force in z direction

Conclusion

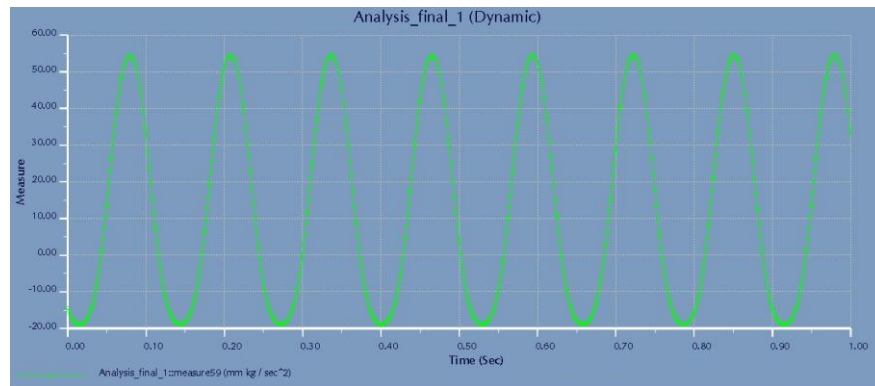Micro air vehicle is a new field of study having wide applications. The Flapping wing mechanism presented in this thesis successfully achieved the task of varying relative flapping frequencies of the wings. A single actuator drives both wings making the design compact. It can introduce or correct asymmetry in flapping frequency of two wings. The sensitivity of the frequency change mechanism can be tuned to reduce the motion and power requirements.

Mechanism was visualized in the light of literature survey, available fabrication facilities and mandate requirement. Mechanism was modeled in software to get approximation of acquired motion of flap. After many alterations model was finalized. The mechanism was mathematically modeled and results compared with commercial codes next step was to go for fabrication of designed mechanism, it was fabricated in local workshop which was the most difficult and hectic task. Designed mechanism was fabricated successfully and experimented to calculate power requirements for the mechanism.

It's Kinematic and Dynamic analysis proves the viability of the design. The results could be used for various kinematic and dynamic applications in the field of MAVs. The prototype assembly can be used for evaluation of power requirements for various wing shapes.

In future this mechanism can me designed with variable flapping amplitudes with provision of variable flapping frequencies to increase the flying efficiency. As mechanism can introduce or correct asymmetry in flapping frequency of two wings it can be implemented with feedback. In future if asymmetry in flapping frequencies proves to be beneficial in certain respect this mechanism can be used with minor alterations.

References

[1] Article "Dragonfly or Insect Spy? Scientists at Work on Robobugs.", Rick Weiss, Washington Post Staff Writer, Tuesday, Washington Post October 9, 2007.

[2] International Symposium on Flying Insects and Robot, Switzerland, August 12-17, 2007.

[3] Design, aerodynamics, and vision based control of the DelFly, G.C.H.E. de Croon, K.M.E. de Clercq, R. Ruijsink, B. Remes, and C. de Wagter, Aerospace Software and Technologies Institute, Technical University of Delft Rotterdamseweg 380, 2629 HG, Delft, the Netherlands.

[4] Design and development of flapping wing micro air vehicle, V. Malolan, M. Dineshkumar and Dr. V. Baskar, Madras Institute of Technology, Anna University, Chennai, India 42nd AIAA Aerospace Sciences Meeting and Exhibit, Reno, Nevada, 5 - 8 January 2004.

[5] Unmanned Aerial Vehicles (UAVs), www.livingroom.org.au.

[6] Naval Research Lab MITE (Micro Tactical Expendable), www.designationsystems.net, 2006.

[7] UAV Forum,www.uavforum.com/vehicles/developmental/blackwidow.htm, 2006.

[8] Design of a Mechanism for Biaxial Rotation of a Wing for a Hovering Vehicle, McIntosh, Sean H., Agrawal, Sunil K., Khan, Zaeem, IEEE/ASME Transactions of Mechatronics, Vol. 11, No. 2, April 2006.

[9] MEMS Wing Technology for a Battery-Powered Ornithopter, Pornsin-sirirak, T., Lee, S., Nassef, H., Grasmeyer, J, 13th IEEE Annual International Conference on MEMS, Miyazaki, Japan, January 23-27, 2000.

[10] Microbat: A Palm-Sized Electrically Powered Ornithopter,by Pornsin-Sirirak, T. Nick., Tai, Yu-Chong., Ho, Chih-Ming., Keennon, Matt., NASA/JPL Workshop on Biomorphic Robotics, Pasadena, CA, 2001.

[11] Isaac, K. M., Colozza, Anthony., Rolwes, Jessica., Force Measurements on a Flapping and Pitching Wing at Low Reynolds Numbers," 44th AIAA Aerospace Sciences Meeting and Exhibit, Reno, Nevada. Sept. 2006.

[12] The development of a miniature flexible flapping wing mechanism for use in a robotic air vehicle, Gautam Jadhav, Georgia Institute of Technology May 2007.

[13] Development of flapping mechanism for micro air vehicle , V. Baskar1 and A. Muniappan2 Proceedings of the International Conference on Mechanical Engineering 2003(ICME2003), Dhaka, Bangladesh 26- 28 December 2003.

[14] Flight Dynamics of a Butterfly-type Ornithopter, Hiroto Tanaka, Kazunori Hoshino, Kiyoshi Matsumoto, and Isao Shimoyam in 2005 IEEERSJ International Conference on Intelligent Robots and Systems 2005.

[15] Debra Rich, Advisor: Dr. S.K. Gupta, Institute for Systems Research, University of Maryland, College Park Summer 2007.

[16] Ornithopter Zone. "Why Flapping Wings" 2007.

[17] Design of a Flapping Wing Mechanism, semester project, Manuel Naef, Stefan Leutenegger Samir Bouabdallah, 2009.

[18] Experiment-Based Optimization of Flapping Wing Kinematics, Scott L. Thomson, Christopher A. Mattson, Mark B. Colton, Stephen P. Harston, Daniel C. Carlson, Mark Cutler, 47th AIAA Aerospace Sciences Meeting Including The New Horizons Forum and Aerospace Exposition , , Orlando, Florida , 5 - 8 January 2009.

[19] Energetic-Based Design of Small Flapping-Wing Micro Air Vehicles, Rajkiran Madangopal, Zaeem Ashraf Khan, and Sunil K. Agrawal, IEEE/ASME TRANSACTIONS ON MECHATRONICS, VOL. 11, NO. 4, AUGUST 2006.

[20] Design and Optimization of a Mechanism for Out of Plane Insect Wing Like Motion With Twist Sai K. Banala, Graduate Student, Sunil K. Agrawal, ,Mechanical Systems Lab, Department of Mechanical Engineering University of Delaware, Newark, DE 19716.

[21] Micro air vehicles–toward a new dimension in flight, McMicheal, J.M., Francis, US

DARPA/TTO Report, 1997.

[22] Quick estimates of flight fitness in hovering animals, Weis-Fogh, including novel

mechanism for lift production. J. Exp. Biol. 59, 169–230, 1973.

[23] Leading-edge vortices in insect flight, Ellington, C.P., Berg, Nature 384, 626–630, 1996.

[24] Wing rotation and the aerodynamic basis of insect flight, Dickonson, M.H. Science 284, 1954–1960, 1999.

[25] Two-color compensation method for measuring unsteady vertical force of an insect in a wind tunnel, Zeng, L., Matsumoto, H., Kawachi, Measurement Science and Technology 7, 515–519, 1996.

[26] Unsteady aerodynamic force generation by a model fruit fly wing in flapping motion Sun, M., Tang, Journal of Experimental Biology 205, 55–70, 2002.

[27] Unsteady lift mechanisms in insect flight. Advances In Mechanics(in Chinese), Sun, M.: 32(3), 425–434, 2002.

[28] The mechanical design of insect wings. Scientific American 263(5), Wootton, R.J.: 114–120 ,1990.

[29] The effects of flexibility on the aerodynamics of moth wings, towards the development of flapping-wing technology, Smith, Michael, J.C AIAA Paper 95-0743, 1995.

[30] Lan Liu, Zongde Fang, and Zhaoxia He, Optimization Design of Flapping Mechanism and Wings for Flapping-Wing MAVs ,School of Mechatronics, Northwestern Polytechnical University, Xi'an 710072, China,2008.

[31] www.gizmology.net/cvt.

[32] Introduction to robotics, third edition John J Craig article 3.2, figure 3.5, page 68.